HIGH RESOLUTION REMOTE SENSING OF EELGRASS (*ZOSTERA MARINA*) IN SOUTH SLOUGH, OREGON

by

RILEY O'DARBY ANDERSON

A THESIS

Presented to the Department of Geography
and the Graduate School of the University of Oregon
in partial fulfillment of the requirements
for the degree of
Master of Science

June 2020

THESIS APPROVAL PAGE

Student: Riley O'Darby Anderson

Title: High Resolution Remote Sensing of Eelgrass (*Zostera marina*) in South Slough, Oregon

This thesis has been accepted and approved in partial fulfillment of the requirements for the Master of Science degree in the Department of Geography by:

Mark Fonstad	Chairperson
Patricia McDowell	Member

and

Kate Mondloch	Interim Vice Provost and Dean of the Graduate School

Original approval signatures are on file with the University of Oregon Graduate School.

Degree awarded June 2020

THESIS ABSTRACT

Riley O'Darby Anderson

Master of Science

Department of Geography

June 2020

Title: High Resolution Remote Sensing of Eelgrass (Zostera marina) in South Slough, Oregon

Eelgrass (*Zostera marina*) supports aquatic biodiversity, carbon sequestration, aquaculture, and water quality. Eelgrass has been undergoing global decline for more than three decades. Lack of spatially extensive, long-term monitoring data is limiting eelgrass conservation and restoration projects, which have low success rates in the Pacific Northwest. This study compares pixel- and object-based image classification techniques on high spatial resolution drone and aerial imagery of eelgrass in South Slough, Oregon. It also quantifies change in spatial distribution and geometry over a three-year period. I find that low-cost imagery can recognize low eelgrass coverage in Pacific Northwest tidal marshes with moderate success. Both classification algorithms overestimated coverage by misidentifying algae as eelgrass and neither consistently performed best for eelgrass mapping. I detected a 44.8% net loss in coverage between 2016 and 2019. Increasing patch shape complexity and fragmentation in areas of decline suggest that disturbances are affecting landscape and patch-level eelgrass factors.

CURRICULUM VITAE

NAME OF AUTHOR: Riley O'Darby Anderson

GRADUATE AND UNDERGRADUATE SCHOOLS ATTENDED:

University of Oregon, Eugene, OR
University of California – Santa Barbara, Santa Barbara, CA

DEGREES AWARDED:

Master of Science, Geography, 2020, University of Oregon
Bachelor of Arts, Geography, 2018, University of California – Santa Barbara

AREAS OF SPECIAL INTEREST:

High resolution remote sensing
Conservation ecology

GRANTS, AWARDS, AND HONORS:

Rippey Award, University of Oregon Department of Geography, 2019

ACKNOWLEDGMENTS

I would like to thank Dr. Mark Fonstad and Dr. Patricia McDowell for their support and guidance throughout these past two years. I would also like to thank the South Slough National Estuarine Research Reserve, namely Ali Helms, Jenni Schmitt, and Shon Schooler, for helping in the development of my field methodology, providing monitoring data and maps, and permitting me to collect data in the estuary. I want to offer sincere thanks to my sister Farlin and my dad for being loyal field assistants in the muddy and windy environment at South Slough.

I wish to express appreciation to the UO Geography graduate student community for their unwavering support and to past and current River Rats for solidarity and technical assistance. Finally, I would like to thank my family, best friends Chelsie and Owen, and my partner Michael for invaluable encouragement during my time in graduate school.

To my papa, who taught me the value of maps, photography, and nature.

TABLE OF CONTENTS

LIST OF FIGURES

LIST OF TABLES

Table Page

CHAPTER I

INTRODUCTION

Background

Seagrasses are a type of macrophyte that present important ecosystem services to their natural environment by sequestering carbon, providing habitat to marine life, and increasing sediment deposition (Waycott et al. 2009). These marine angiosperms consist of 72 species and are found on every continent except Antarctica (Short et al. 2011). Researchers have estimated 29% of seagrass cover has been lost since the late 1800s, with prominent loss occurring within the genus *Zostera* (eelgrass) (Waycott et al. 2009). *Zostera marina* is a species native to the coasts of North America and Eurasia, where it serves as a carbon sink and nursery habitat for salmon in the Pacific Northwest Phillips 1984). More frequent and in-depth monitoring of this declining species is thus critical. This thesis tests the use of remote sensing using low-cost, consumer-grade imagery acquired from an unmanned aerial vehicle and free aerial imagery from the National Agriculture Imagery Program in order to improve eelgrass monitoring.

Aside from its recent decline, eelgrass is a popular species within conservation given its array of ecological benefits. Eelgrass beds on an ecosystem level are indicators of the ecological health of estuarine habitat (Rumrill and Sowers 2008). They are a foundation species that improves water quality, prevents coastal erosion, shelters breeding fish and invertebrates, and reduces current and wave velocity (Waycott et. al 2009). As with other seagrasses, eelgrass displays itself along a gradient, ranging from highly fragmented, small, sparse patches to dense, large, and continuous ‘meadows’.

This species in particular needs to be prioritized due to its rapid decline that began in the 1980s (Short et al. 1987). Suggested drivers of the decline are many: coastal development, increased turbidity and water temperature, presence of green crab (*Carcinus maenas*), geese grazing, eutrophication, eelgrass wasting disease, macroalgae, and dehydration from tidal patterns and insolation. Eelgrass decline across the globe is not understood yet and thus, a standard in monitoring procedures and environmental variables has not been established, leaving it up to each agency to decide. Field measurements using percent coverage and shoot density estimates within quadrats are the most common monitoring method, yet monitoring via airborne imagery and sonar are becoming common for their ability to capture larger spatial extents.

Sparse eelgrass requires more attention and is becoming more common as eelgrass habitats decline in quality. In undisturbed environments, patches of eelgrass typically grow into meadows; when conditions prevent patches from expanding or cause meadows to fragment, the patches have higher sensitivity to environmental limiting factors than eelgrass meadows. The rhizomes of patchy eelgrass are more susceptible than continuous eelgrass meadows to negative effects from invasive marine species such as the introduced mussel *Musculista senhousia* or green crab (Reusch and Williams, 1997). Small patches are more likely to be lost to a state of bare sediment from being pushed beyond the state threshold by both bioturbation and disturbance from wave velocity (Uhrin and Turner 2018, Carr et al. 2010). The spatial distribution of eelgrass rhizomes also affects monitoring accuracy: measuring depth limits, which is an indicator of the health status of the seagrass, has higher uncertainty when done in patchy areas due to divers having different depth estimates when crossing the depth limits at different

locations (Balsby, Carstensen, & Krause-Jensen 2013). Smaller spatial units of aquatic vegetation are distinguished less often than large meadows and sometimes omitted entirely when using low-resolution satellite and aerial imagery for detection (Nahirnick et al. 2018).

The urgency to conserve seagrass habitats has inspired a variety of in situ monitoring methods, such as scuba surveys (Whippo et al. 2018), standardized ground-based sampling for citizen-science efforts (Seagrass cit), and hovercraft-based mapping (Mckenzie, 2003). Remote sensing approaches are now common for estimating seagrass coverage and density: active acoustic remote sensing, like side scan sonar, and passive spectral sensors that are used on boats and kayaks (Nahirnick 2018), manned and unmanned aircraft (Duffy et al. 2018), or satellites. While habitat mapping of coastal wetlands using low spatial resolution imagery, such as Landsat (25m resolution), has been done before (Ward et al. 2003), higher resolution aerial imagery has been the standard data format for mapping eelgrass, as more complex, fragmented seascapes are delineable and timing of image acquisition is more flexible (Costello and Kenworthy 2011, Uhrin and Turner 2018, EPA 2007). Furthermore, the usage of unmanned aerial vehicles (UAVs), commonly known as drones, are becoming increasingly preferable among conservation groups due to their relative low cost, flexibility of flight planning, and ability to capture eelgrass health indicators at fine scales (Duffy et al. 2018, Ventura et al. 2018).

Advancements in land cover classification techniques are also improving conservation mapping. Namely, object-based image analysis (OBIA) is now often used in high resolution remote sensing of complex landscapes because the objects of interest are

made up of multiple pixels, compared to pixel-based classification techniques applied to coarser spatial resolution data that represent multiple objects within one pixel. OBIA first groups pixels that are spectrally similar and spatially close into "objects" before classifying the scene, which can assist in studying vegetation patch dynamics, such as patch size, shape complexity and internal gap dynamics (Nahirnick et al. 2018, Barrell et al. 2015). Efficient means of studying landscape metrics in eelgrass habitats are important to establish, as they may indicate an irreversible equilibrium shift (Uhrin and Turner 2018, Carr et al. 2010). This research applies high resolution aerial imagery and OBIA to eelgrass habitats in South Slough, Oregon, USA for identification of present eelgrass and detection of changes within patch dynamics.

Study Site

South Slough (43°20' N, 124°19' W) is a tidal inlet at the mouth of Coos Bay, Oregon. The estuarine subsystem is located within the Coos watershed (467,200 acres) and the 5900 acre South Slough National Estuarine Research Reserve (SSNERR), established in 1974. As part of the drowned river mouth Coos estuary, the slough consists of sand and mudflats and salt marshes that border an open water tidal channel. The mean tidal range at the mouth of Coos Bay is 2.3m, with the highest tides 3.3m above mean lower low water (MLLW) and lowest tides occurring at -0.9m below MLLW (Rumrill 2015). Similar to other regions of the Pacific Northwest, eelgrass and benthic macroalgae exist as the dominant submerged aquatic vegetation in the low intertidal zone of the wetlands, while more diverse assemblages of emergent vegetation inhabit the middle and upper intertidal zones (Rumrill 2008). Salinity ranges from marine to riverine values, with distinct hydrographic regions existing within the slough. Historically, eelgrass could

be found in dense meadows in the marine and polyhaline regions, as well as the riverine/mesohaline region. Only sporadic 1-3 m^2 patches were found in the oligohaline regions of the estuary (Rumrill 2008).

Monitoring sites for eelgrass, established by researchers at SSNERR, were chosen to reflect the variety of ecologic and hydrographic conditions at eelgrass sites within the slough. The four existing monitoring locations were used as sites for this research (Figure 1).

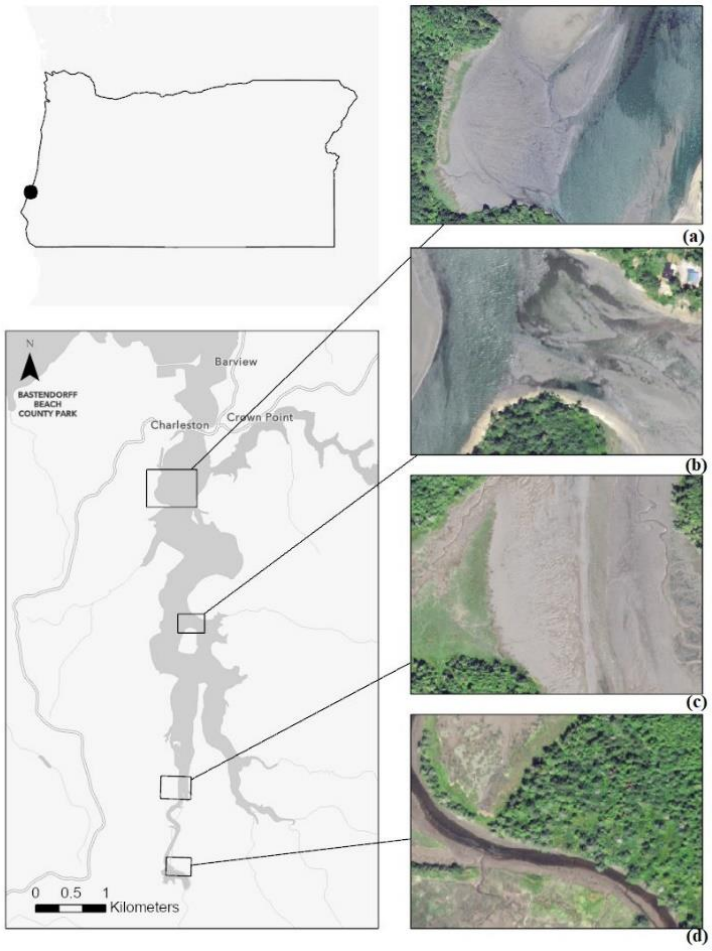

Figure 1. Map of South Slough, Oregon (left) and the SSNERR eelgrass monitoring sites (right) represented by 2016 NAIP 1m aerial imagery. From a-d: Collver Point, Valino Island, Hidden Creek, and Danger Point.

The monitoring sites have permanent transect lines throughout the historic eelgrass extent and are accessible by foot. The accessibility of these sites was a major determining factor in where imagery was collected because the upstream reaches of the slough cannot be navigated by boat or kayak at lower tides and the UAV battery life and Federal Aviation Administration (FAA) rules did not allow for launching flights from hundreds of meters away. By selecting these sites with long-term monitoring data, I was also able to assess the accuracy of eelgrass classification in aerial imagery from 2016 (Chapter 2).

Collver Point (43°19’47" N, 124°19’8" W), in the marine-dominated region, is a sandstone headland with a silty salt marsh, adjoining mudflats and cobble terrace. Eelgrass beds are a fringe along the edge of the tidal channel. Valino Island (43°18’50" N, 124°19’5" W), in the polyhaline region, is the only site of four sites that has expansive sandy tideflats. Eelgrass meadows have historically spread out across the sandflats, while also fringing along the edge of the deep tidal channel. Hidden Creek (43°17'28" N, 124°19'16" W) is the third monitoring site and consists of a silty, mesohaline salt marsh and eelgrass patches fringing along the tidal channel. Lastly, Danger Point (43°16’58" N, 124°19’17' 'W) is in the riverine region of the upper
estuary, where a narrow tidal channel passes by mudbanks and a high salt marsh. An eelgrass bed historically existed along the length of the channel.

Two sites, Hidden Creek and Danger Point, have been without eelgrass since 2017. They were included in the research to test how image resolution and classification methods affect the classification accuracy on landscapes within the South Slough that do not have eelgrass.

Research Questions

This research seeks to test the effectiveness of two different image classification techniques, pixel-based unsupervised and supervised classification and object-based supervised classification, on eelgrass via aerial imagery of varying high spatial resolutions in South Slough. It also aims to analyze the change in the spatial metrics of eelgrass patches in South Slough from 2016 to 2019. Effective monitoring techniques are needed in South Slough and other areas experiencing major eelgrass declines in order to increase knowledge of eelgrass spatial ecology to better prevent and mitigate net losses. Furthermore, given that both UAVs and OBIA are emerging, hot topics within conservation mapping in this current day, it is important to understand how they can benefit eelgrass mapping. The overall research questions in this thesis are as follows:

Question 1: How effective are classification techniques (unsupervised, supervised, OBIA) in mapping sparse intertidal eelgrass in South Slough, Oregon with UAV imagery?

Question 2: How accurate is National Agiculture Imagery Program (NAIP) imagery in mapping eelgrass in South Slough, Oregon?

Question 3: How has eelgrass distribution in South Slough, Oregon changed from 2016 to 2019?

CHAPTER II

MAPPING EELGRASS FROM UAV IMAGERY WITH THREE IMAGE CLASSIFICATION TECHNIQUES

Introduction

Unmanned aerial vehicles (UAVs) have recently come into the conservation spotlight as a solution to the operational issues that come with species distribution mapping and monitoring. Historically used for military purposes, the 2010s welcomed new drones that have been manufactured in small, lightweight forms and are being sold at relatively low costs. UAVs are able to tackle the three most common obstacles in using remote sensing for conservation efforts: high spatial resolution needs, ability for frequent repeat flights, and imagery acquisition costs. Along with other agencies and organizations, the National Oceanic and Atmospheric Administration has recognized the potential for UAVs, stating that they "have the potential to efficiently and safely bridge critical information gaps" in data-sparse locations "and advance understanding of key processes in Earth systems" (NOAA 2012).

The use of UAVs for mapping is of particular interest to seagrass conservationists. Satellite imagery, especially in temperate coastal regions, is susceptible to cloud coverage and variable tide states that affect the ability to identify seagrass and perform time-series investigations. Even with fine spatial resolution satellite data, individual seagrass plants and shoots are not identifiable (Duffy et al. 2018). With pressure to monitor seagrass habitats more frequently, conservationists cannot rely upon aerial imagery from annual aircraft missions such as the National Aerial Imagery

Program from the USDA's Farm Service Agency due to the risk of poor environmental conditions (cloud cover, tidal state) that satellite imagery also harbor. Mapping of seagrass done "in the field" by UAV/spectroradiometer, or other form of photograph, was the fourth most utilized remote sensing approach in a 2015 review, comprising 14% of the published studies on seagrass mapping (Hossain et al. 2015).

Publications on eelgrass mapping via UAVs have arisen only since 2016. The only publications to focus primarily on eelgrass mapping have involved testing the effects of environmental conditions on mapping quality (Nahirnick et al. 2019) as well as comparing the performance of different classification approaches (Duffy et al. 2018). Nahirnick et al. (2018) classified patchy eelgrass as having a “low mapping confidence level” but concluded that ideal environmental conditions would allow for high confidence mapping of sparse eelgrass, while Duffy et al. (2018) found their more sparse site to be more accurately classified than a densely vegetated site. As eelgrass declines globally, many coastal estuaries may already have low percent cover of eelgrass. The applicability of UAV mapping in areas undergoing rapid declines in eelgrass coverage is still unknown. To advance knowledge surrounding eelgrass mapping, this research tested different classification approaches on UAV imagery in South Slough, Oregon, USA, where recent years have seen rapid declines in eelgrass cover (Wirfs and Helms, 2018).

Ground Data Collection

Permanent transect lines exist at all four monitoring sites. The lines run from the upland-marsh boundary (about +2.6m mean lower-low water (MLLW)) to the marsh-mudflat boundary (about +1.4m MLLW). However, at Collver Point, the lines do not

meet the salt marsh transect as there are 90-110m of mudflats in between. The 50-100m lines at all sites are identified by stakes that mark ~20 0.25-m^2 evenly spaced quadrat plots. I was unable to monitor at the majority of permanent plots due to the water being too deep for accessibility, as some plots are not exposed at low tide during certain periods of each month. Instead, I followed the same monitoring protocol by randomly sampling at accessible (i.e. exposed) locations using a 0.25m^2 PVC quadrat. Per the Seagrass-Watch protocol (Mckenzie et al. 2003), I visually estimated the percent coverage of eelgrass, algae, and substrate at 5% cover intervals at nine randomized quadrats at the two eelgrass sites (Valino Island and Collver Point). Although this protocol naturally has uncertainties, it is the method deployed for all eelgrass monitoring done in South Slough by SSNERR and is presumed to be "truth" for the purpose of this study. I used a Trimble Geo7x GPS to collect the GPS coordinates of each corner of each quadrat; these coordinates were also used for calculating the spatial accuracy error in the GPS data derived from the UAV. Although my sampling locations were randomly chosen, a weakness in this approach is that the samples are biased towards water-free locations in the site. The seasonal monitoring done by SSNERR at their permanent plots was included to add more validation points in the accuracy assessment done post-classification.

UAV Flight Planning and Implementation

Flight planning for UAVs over coastal eelgrass habitat must take into consideration wind speed, tidal height, cloud cover, turbidity, and sun angle. Ideal conditions for high confidence eelgrass mapping consist of: wind speeds below 5 $km \cdot h^{-1}$, <10% or >90% cloud cover, Secchi depths over 5m, and sun angles below 40° (Nahirnick

et al. 2019). Furthermore, the phenology of eelgrass renders the flowering periods in late spring and early summer to be the best time for mapping, as eelgrass biomass and density is most abundant then. The flight conditions are detailed in Table 1.

I piloted a DJI Phantom 3 Professional with its 4K camera, DJI FC300X, for this study. The camera has 12.4 effective megapixels, an image size of 4000 x 3000 pixels, a sensor size of 6.17 x 4.55mm, and a lens IFOV of 94°. For the bright conditions of the estuary, I programmed the camera with an ISO of 100, f-stop of f/2.8, and shutter speed of 1/2500 sec. The number of photos collected at each site ranged from 200 (Danger Point) to 900 (Collver Point). The number of flights required to cover the sites ranged from 2 to 6 (Table 2).

Table 1. Summary of environmental conditions by site. Turbidity and water depth values were taken from the closest water quality and weather monitoring stations to each site within South Slough (NERRS 2020).

Site	Date	Time	Sun angle	Water depth (m)	Wind speed (m/s)	Cloud cover	Turbidity (NTU)
Danger Point	6/30/19	8:45-9:15 am	30°	1.16	2	75%	20
Hidden Creek	7/14/19	8:45-9:45 am	29°	1	0.3	10%	18
Valino Island	7/30/19	7:30-8:30am	13°	1.07	0	5%	5
Collver Point	8/1/19	7:00-8:30am	8°	0.57	0	5%	4

At Collver Point, Valino Island, Hidden Creek, and Danger Point, I collected RGB images at 10m and 20m above ground. A preliminary study done on UAV eelgrass

mapping in Coos Bay recommended flying at ~20m (Earth Design 2019). The report showed that flights at ~20m had higher spatial accuracy than ~10m flights and required less computational and data processing time than smaller images, yet image quality was best at ~10m (Earth Design 2019). Additionally, simply repeating my flights increased the chances of having imagery viable for structure from motion processing.

Flight plans allow for image capture speeds, camera orientation, and UAV speed and path to be programmed into the device for easier flying, however poor GPS signal can cause the UAV to diverge entirely from the flying area (personal observation). The option of a flight plan for automated flying was dismissed prior to fieldwork, as housing along the water and thick riparian forest at the study site made any accidental digression from the estuary too dangerous. Consequently, I manually captured images every one to two seconds and maintained a 75% overlap between flight paths with the help of a visual observer. Overlap of successive images by at least 80% and parallel images by 60% is necessary for structure from motion processing to mosaic photos together through common points.

Structure from Motion (SfM) Processing

I used Agisoft Metashape Professional v.1.4.3 to create orthophotos from the images taken during the UAV flights. Agisoft Metashape Professional is a commercial-grade structure from motion software that builds 3-dimensional data from common points within photographs. After removing blurry images, I aligned the photos in the software. I tried re-alignment of both the whole set of photos and certain batches of photos in order to increase the percentage of aligned photos. Alignment of all photos was not possible at

any of the sites; the homogeneity of features in wetland environments (water bodies, bare sand) makes it difficult for structure from motion software to detect the orientation of photos for alignment when no identifying marks such as rocks or eelgrass are present. Even when sufficient overlap was achieved, aquatic portions of some scenes were deemed unviable for mosaicking because environmental conditions such as sun glint, ripples in the water surface from wind, and high turbidity made overlapping regions of images appear nonidentical due to temporal heterogeneity. Images from high tide scenes consequently had to be omitted from this research. Even at low tide I was not able to process an orthophoto from Danger Point due to low photo counts and spectral properties in the narrow, low-velocity site. For scenes that successfully generated a sparse point cloud, I removed any points in the resulting sparse point cloud that were registering as outliers. Although 10m flights at Valino Island and Collver Point produced quality comparable to the 20m flights, the 20m imagery lost significantly less area at the edges than the 10m imagery, which led me to choose 20m imagery for the image analysis (Table 2). The dense point cloud and mesh were created from this sparse point cloud. The orthophotos were generated after these steps (see Figure 2).

Table 2. Flight specifics for each site.

Site	**Height above ground (m)**	**Avg. flight speed (km/hr)**	**Area (ha)**	**Flights**	**Spatial resolution (cm^2)**
Hidden Creek	20	10	2.4	3	3.9
Valino Island	20	10	3.2	4	3.9
Collver Point	20	10	7.65	6	3.9

The individual JPEGs used for generating the orthophoto have a spatial accuracy equal to the accuracy of the GPS onboard the UAV, which captures spatial information in the WGS-84 coordinate system. Ground control points taken from the quadrat monitoring were used to calculate error in spatial accuracy. I projected the orthophotos into NAD-83 UTM Zone 10 for two reasons: to match imagery flown in 2016 (see Chapter 3) and calculate minimum mapping units and other spatial geometries with minimal distortion. The spatial resolution of each orthophoto was resampled to 25cm² to decrease computing requirements and match 2016 aerial imagery for further comparisons, while the spatial accuracy of the orthophotos was calculated as 60cm^2 after comparison to the in-situ quadrat sampling. The application of a minimum mapping unit (MMU) during classification solves the difference in these resolutions.

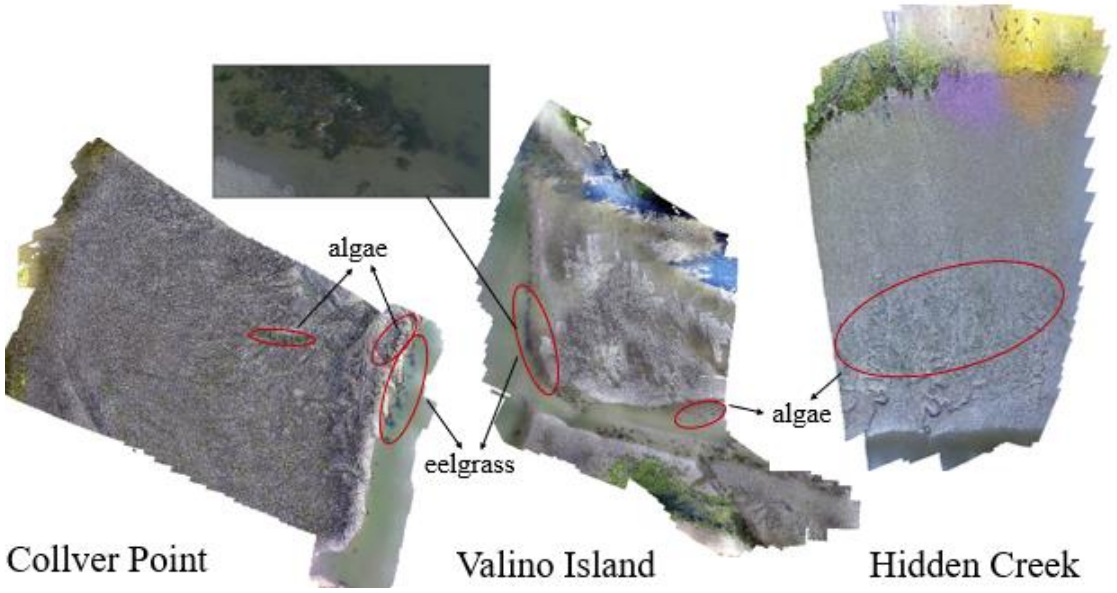

Figure 2. UAV orthophotos of the three monitoring sites, with eelgrass and algae highlighted. Hidden Creek is a control site with no eelgrass present.

Classification

The classification schema for all sites consisted of four classes. At eelgrass sites, the classes were: substrate, water, eelgrass, and algae. At the algae-only site, the classes were instead substrate, water, riparian vegetation, and algae. Riparian vegetation was present at all sites, yet minimal differences in accuracy when riparian vegetation was included separately or within the algae class removed the need for a fifth class. During the beginning stages of segmentation and/or training, substrate was split into dry and wet substrate classes and eelgrass was differentiated by submerged and exposed eelgrass. At Hidden Creek, riparian vegetation was first identified as healthy vegetation and grasses to reduce spectral overlapping between riparian plants and algae.

I used ArcGIS Pro v2.1.4. for all image classification techniques. First, I performed unsupervised classification on Hidden Creek, Collver Point, and Valino Island orthophotos. Basic unsupervised classification on true color imagery reveals what level of classification can be achieved when no reference data or band algebra is used to train the classifier. I performed this work with iso cluster unsupervised classification, which combines maximum likelihood classification and a modified iterative optimization clustering procedure. The only parameters set by the user are the number of classes, maximum iterations, maximum cluster merges, merge distance, minimum samples per cluster, and the skip factor. The iterations assign samples to clusters and assumes that the statistics for each class in each band are normally distributed (ESRI).

The second classification technique was supervised classification using a support vector machine classifier. Supervised classification uses training samples to assign pixels to classes within the user's specified classification scheme. When creating training

samples, each class contained ~300 pixels, following the remote sensing principle that if *n* is the number of bands in the image, training classes should contain pixels between 10*n* and 100*n*. I used a support vector machine (SVM) classifier for this method because SVM is known for being able to handle larger images than random forest classifiers and is less susceptible to noise and the number or size of training samples (ESRI).

Using high spatial resolution remote sensing for classifying vegetation does not always benefit classification accuracy or performance. Due to the increase in spatial resolution, the spectral variability of classification targets can increase, which directly reduces the statistical separability between classes with traditional pixel-based classification. This can cause noise in the image (the "salt-and-pepper effect") where pixels of one vegetation class are assigned different classes. Deemed the "H-resolution problem", various pixel-based improvements have been developed, such as post-classification processing to decrease noise through filtering, contextual classification, or pre-processing with filtering and texture analysis (Woodcock and Strahler 1987). Yu et al. (2006) point out that these solutions have apparent disadvantages when utilized for high spatial resolution images up to 10 m: 1) the pre-defined neighborhood window size does not address the different pixel window sizes that different land cover classes require, 2) the high computational needs of these processes favor large window sizes, and 3) accuracy is still low for boundary pixels.

Object-based classification, also more commonly grouped into object-based image analysis (OBIA), is a popular alternative to pixel-based classification because it addresses the H-resolution problem (Gamanya et al., 2009). OBIA is derived from segmentation, edge-detection, feature extraction and classification concepts that have

been used in remote sensing image analysis for decades (Blaschke 2010), but was not used extensively in geospatial applications until the 21st century (Blaschke et al. 2004). By segmenting objects of interest by spatial and spectral proximity, OBIA can eliminate the salt-and-pepper effect in high spatial resolution images that can be caused by shadows, gaps, or textures.

Updates to the image classification tools in ArcGIS Desktop products in recent years have introduced traditional OBIA parameter setting by scale, shape, and compactness (ESRI 2020, Kavzoglu & Yildiz 2014). ArcGIS Pro uses the machine-learning classifiers (random forest and support vector machine) as a less interventive and scene-specific alternative to rule sets that are used in other OBIA software. However, finding optimal parameter settings required applying a trial and error approach to each individual scene - a tedious but common method that is used in many OBIA projects where open-source segmentation parameter optimization code is not available (Zhang, Fritts, and Goldman 2008). Within the segmentation parameters, spatial detail (compactness), spectral detail (shape), and minimum segment size (scale) need to be set by the analyst. The spectral detail parameter determines how much influence the spectral characteristics of pixels have on segmentation; a high value is best for objects of interest that have similar colors, such as algae and eelgrass. The spatial detail parameter prioritizes the proximity of features and a higher value results in objects that are more clustered together. The minimum segment size parameter controls the scale of the objects, which allows analysts to set a constant MMU for the scene.

The spectral detail parameter for all three sites was set to 19 (on a range of 0-20), because spectral separability of eelgrass, algae, and riparian vegetation was low. The

spatial detail was set to 15 (on a range of 0-20) for Collver Point and Hidden Creek and 19 for Valino Island. The majority of algae was meters apart from eelgrass at Collver Point, and thus segmentation of objects was most realistic with a spatial detail setting of 15; higher values separated eelgrass patches into multiple objects. Algae and eelgrass were typically less than a meter apart at Valino Island, so a value of 19 for spatial detail was most ideal.

I assessed the accuracy of the three algorithms by comparing the reported eelgrass coverage of randomly selected points to the real-life eelgrass as documented in the SSNERR and pre-flight field monitoring. Half of the monitoring quadrats were used for creating the training samples, while the other half were utilized as validation points. Random automation of accuracy assessment points resulted in 80 accuracy assessment points per site, of which I manually classified the true land cover class. The same stratified random sampling design was applied for both pixel- and object-based classifications. Monitoring data from SSNERR validated points that fell along the permanent sampling transects, while other points were interpreted using visual inspection. Visual inspection of high spatial resolution imagery is actually quite reliable for assessing accuracy (Lechner et al. 2012, Nahirnick et al. 2018).

The effectiveness of the classifications was measured by computing accuracies in the form of a confusion matrix. The confusion matrices included producer's accuracy, user's accuracy, overall accuracy, and the Kappa statistic. I did not focus on the Kappa statistic and overall accuracy in the effectiveness of mapping eelgrass because the two values take into account the user's and producer's accuracies of all classes in the classification schemes. The user's accuracy is determined by the proportion of correctly

classified pixels/objects within the total number of samples classified. Contrastingly, the producer's accuracy is the proportion of correctly classified pixels/objects out of the validation points.

Although the accuracy was quantified using only the user's and producer's accuracies, I discuss errors in the classifications in terms of omission/commission errors and Type I/II errors. An omission error occurs when a pixel/object of a certain class is omitted from the correct class; this can also be associated as a Type II error because it is a false negative. Errors of commission are seen when pixels/objects are included into a class that they are not part of in reality (i.e. Type I – false positive error). 1 – user's accuracy will reveal the Type I error (false positives) present in the classification, while 1 – producer's accuracy will reveal the Type II error (false negatives).

Results

The results of the analysis are summarized in Table 3 and illustrated in Figure 3. Figure 2 showcases examples of eelgrass and algae spectral characteristics in the unclassified orthophotos, as the two vegetation types are difficult to distinguish with an untrained eye. Following, each site is addressed individually. Overall, SVM supervised classification performed best at two of three sites, with OBIA classification ranking second.

Hidden Creek

Imagery was acquired at Hidden Creek as a control site, to explore how effective classification techniques are on high resolution UAV imagery when aquatic vegetation consists of solely one genus instead of two or more. At low-tide, this site consists of bare

substrate divided by small gullies connecting Hidden Creek to the tidal channel. Flat layers of microalgae are clustered along the edges of these depressions and decrease in cover from the tidal channel to riparian banks.

Table 3. Accuracy results for eelgrass at each site and algae at the control site. Shaded gray cells indicate the most effective classification technique for eelgrass/algae at a site.

Site - Class	Classification technique	Producer's accuracy	User's accuracy	Average site accuracy (P/U)
Valino Island - Eelgrass	Iso cluster unsupervised	100%	10%	100/13
	SVM supervised	100%	20%	
	Object-based SVM	100%	10%	
Collver Point - Eelgrass	Iso cluster unsupervised	50%	10%	50/10
	SVM supervised	0%	0%	
	Object-based SVM	100%	20%	
Hidden Creek - Algae	Iso cluster unsupervised	100%	16%	98/58
	SVM supervised	100%	80%	
	Object-based SVM	94%	80%	

The imagery collected on July 14, 2019 revealed peculiar yellow and purple spectral displays (see Figure 2) in a portion of substrate after SfM processing. This affected all three classification performances, as the classifiers misclassified substrate as water and riparian vegetation in purple-toned and yellow-toned substrate. Since this did not affect classification of the main class of interest (algae), this issue was not pursued further. Similar to Valino Island results, an SVM classifier used with supervised classification was most effective for mapping algae, with only a 20% error of commission. Notably, OBIA was comparable in terms of effectiveness, with a 20% error

of commission and 6% error of omission. The classifiers dominantly overestimated algae in what was truly wet substrate. The iso cluster classifier found ‘algae’ in turbid water and healthy riparian vegetation, which resulted in a low probability that the mapped microalgae existed in those spaces in real life (16%).

Overall, the average accuracy among the three classifications at Hidden Creek was the highest compared to the eelgrass sites. The classifiers correctly classified accuracy assessment points that were algae and struggled moderately to separate shadows, turbid water, and dark riparian vegetation from algae. While the lack of false negatives was comparable to Valino Island’s high producer’s accuracy, the average user’s accuracy was 58%, whereas sites with eelgrass were 10% and 13%. In terms of spatial variation in accuracy, errors arose most along the transition of mudflats to riparian banks where algae was overestimated in small depressions of water.

Valino Island

The scene at Valino Island consisted of a patchy eelgrass bed along the tidal channel, extensive macroalgae along the shoreline of Valino Island, and sparse eelgrass and algae along the shore of the mainland (Figure 2, Figure 3). The lighter spectral composition of sandflats at this locale showed less contrast between submerged and exposed substrate, resulting in less of the glint that was common at Collver Point and Hidden Creek mudflats. Minor stitching errors from SfM processing (blurring, holes) occur only onshore within the tree canopy.

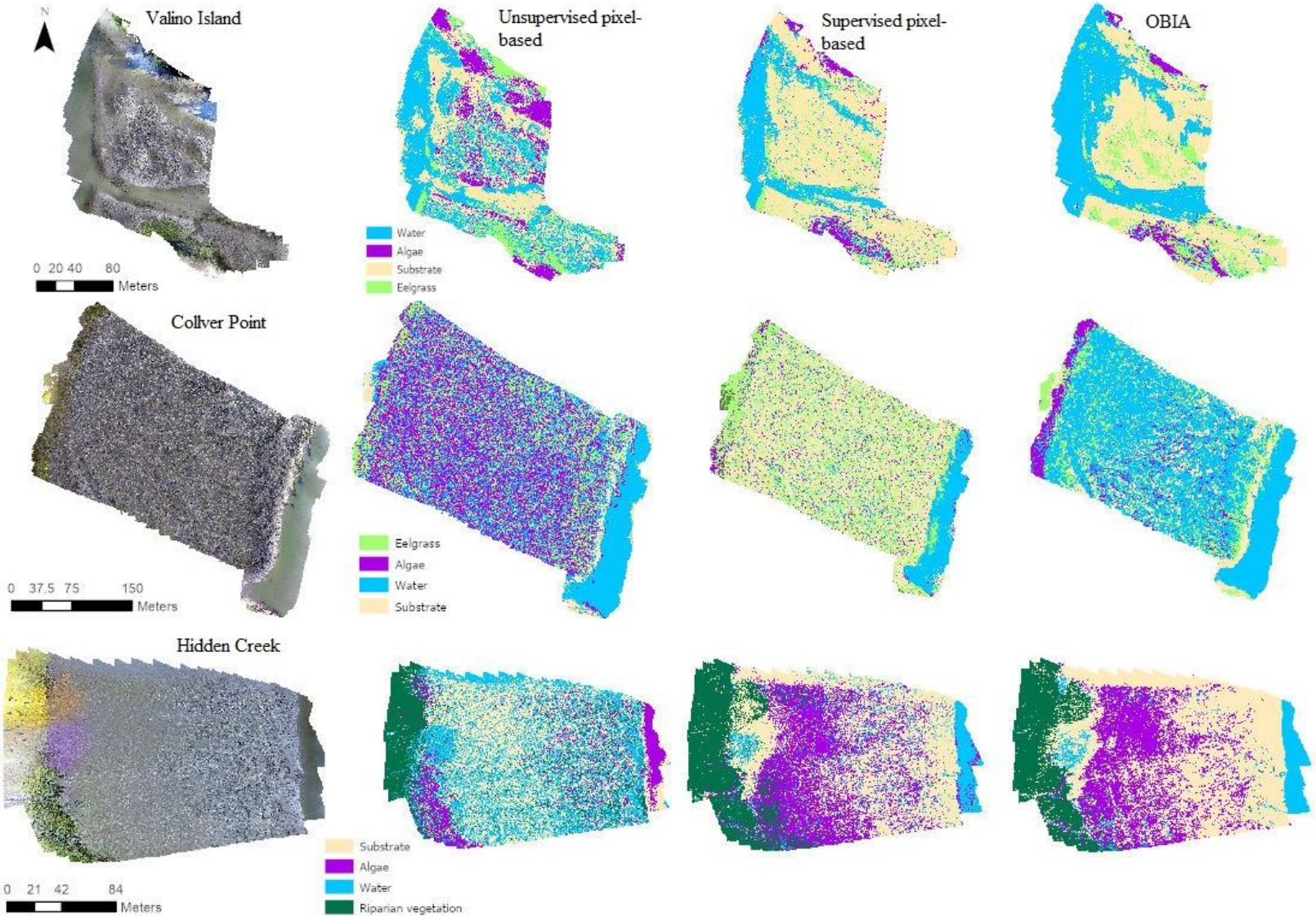

Figure 3. RGB orthophotos and classification results for Valino Island, Collver Point, and Hidden Creek.

Classifiers performed more effectively on eelgrass at Valino Island compared to eelgrass at Collver Point. No Type II errors in eelgrass resulted from any classifiers. However, the high producer's accuracy does not accurately portray the failure of all classifiers, most noticeably the iso cluster, to map the submerged eelgrass that surrounded the eelgrass bed in the deep tidal channel. Further, false positives were relatively similar among classifiers, with only 20% of eelgrass in the SVM supervised classification and 10% of eelgrass in unsupervised and OBIA classifications existing on the ground. The areas in which macroalgae was misclassified as eelgrass - the primary driver of high Type I errors in this scene - occurred in the same places for all classifiers.

Collver Point

Similar to Hidden Creek, Collver Point has extensive mudflats that create issues among water, substrate, and SAV separation. Overall, the SVM supervised map displays the most realistic rendering of land cover classes at CP due to the misclassification of substrate as algae or water by other classifiers (Figure 3). Ironically, this pixel-based supervised classification performed the worst of all nine classification tests, with high Type I and II errors in the eelgrass class (Table 3). Not reflected in the official accuracy assessment, the supervised classification did map true eelgrass in the tidal channel. However, the patches were so small that there was a low likelihood of the random assignment of accuracy assessment points choosing pixels in these outliers. Conversely, the isolation of eelgrass in the tidal channel benefitted OBIA and iso cluster classifiers, as the fragmented bed was less affected by reflection and spectral overlapping on the muddy substrate.

OBIA performed most effectively at this site. Errors of omission were low, but misclassification of macroalgae as eelgrass persisted as an issue. While majority eelgrass at Valino Island was submerged and had less variation in spectral responses, eelgrass patches here varied from dark patches in the deep channel to bright, dry patches along the bank of the channel. The near-white reflections in these shoots potentially caused the overestimation of eelgrass in bright, wet substrate throughout the marsh when training samples were used. The small glints were not represented in OBIA given the nature of segmentation.

Discussion

Moderately high success of each classification technique at the "control" site, Hidden Creek, reveals difficulties in mapping tidal marshes regardless of eelgrass presence. Darker spectral responses from depressions and small puddles in the substrate frequently were misclassified as algae; the salt-and-pepper effect was not solved but amplified with OBIA. The complex heterogeneity of mudflats make mapping with RGB imagery difficult and would likely fare better with multispectral imagery (Tuxen et al. 2007). Nonetheless, accuracy assessment from Hidden Creek suggests that RGB vegetation classification done at non-eelgrass inhabited areas of the South Slough would be less erroneous and more effective than areas with mixed SAV (Table 3).

The errors of commission in South Slough can be seen in the contrasting high producer's and low user's accuracies for Valino Island and Collver Point (Table 3). The OBIA and supervised classification of Collver Point vastly overestimated eelgrass cover, portraying eelgrass abundantly in the mudflats above the tidal channel where algae and

shadows in the substrate depressions were (Figure 3). Even when the segmentation results made the classifications appear more realistic, issues less visually noticeable, such as improperly defined edges between eelgrass and non-eelgrass objects or small patches of algae being classified as eelgrass, brought down the accuracy of the classification at Valino Island and Collver Point. Unsupervised classification successes comparable to OBIA performance in eelgrass mapping have been observed before and may be due to the double-edged sword of "supervision" (Duffy et al. 2018). It is possible that the choice of training segments prior to segmentation contributed to the OBIA performance, given the subjectivity of OBIA (Duffy et al. 2018).

The overestimation of eelgrass through misclassification of non-eelgrass also was reflected in pixel-based classification. User accuracies for eelgrass classification at Valino Island (10-20%) and Collver Point (0-20%) are significantly lower than the user accuracies for algae at Hidden Creek (16-80%). While algae was distributed across the mudflats at Hidden Creek, eelgrass was sparsely clustered at Valino Island and Collver Point, which naturally resulted in an overestimation of coverage at these sites. Since user's accuracy for eelgrass generally failed to improve significantly once classification was 'supervised' with training samples, one can assume that spectral differences between eelgrass and other vegetation were not great enough for high accuracy mapping using solely RGB imagery. If UAV eelgrass mapping were repeated in South Slough, low tide imagery should be attempted with multispectral remote sensing, which can be done using cheaply available consumer grade technology (Baldwin 2019).

Improvements in classification technique and imagery acquisition could make low-coverage eelgrass mapping more successful. Given that textural clues helped visual

interpretation of the scenes, the inclusion of textural layers within supervised classification could increase classification accuracy. Textural layers did not improve uncertainty values of supervised classification in eelgrass meadows in Wales, UK, but pixel-based texture calculation is susceptible to the boundary problem and combining texture analysis and OBIA has increased accuracy of sub-decimeter resolution UAV imagery (Duffy et al. 2018, Laliberte and Rango 2009). The addition of more spectral layers (e.g. near infrared) can further distinguish aquatic vegetation from substrate at low tide, especially because of the spectral complexity of leaves of *Zostera* species (Bargain et al. 2013).

With OBIA performing better on just one of two eelgrass sites, this research mildly supports OBIA as a solution to the so-called H-resolution problem for eelgrass mapping. The overall findings more strongly support the emerging consensus in seagrass mapping that subjectivity and lack of standardization within OBIA workflows are a significant problem (Duffy et al. 2018, Ventura et al. 2016). The analysis will likely vary even among experienced analysts (Hulet et al. 2014). The recent creation of a segment parameter optimization tool that runs in an unsupervised manner in open-source OBIA mapping attempts to make a more objective parameterization process, although no standard, statistically correct procedure for accuracy assessment of segmented maps exists yet (Grippa 2016, Hossain 2016).

Overall, classification technique effectiveness in this study reflects both issues of overestimation and underestimation of eelgrass. Nahirnick et al. (2018) and Barrell and Grant (2015) defined the underestimation of sparse eelgrass cover as the dominant error in their accuracy assessment. The omission errors at Valino Island and Collver Point

occurred primarily in submerged eelgrass, where the spectrally darker eelgrass masses were misclassified as water. Contrastingly, Nahirnick et al. (2018) had few issues with dense eelgrass and more issues with sparse eelgrass being mistaken for sparse macroalgae. While sparse eelgrass was originally expected to decrease effectiveness of classifiers in this research through omission errors, ultimately, the overestimation of eelgrass was the dominant error in classification of South Slough monitoring sites. This highlights the importance of semantics (i.e., what is the definition of 'sparse'?) within conservation GIS and the need for standardization of seagrass mapping.

Eelgrass was mapped in two long-term eelgrass monitoring sites in South Slough, Oregon, USA using three different image classification techniques. Varying sun angles and class distributions at each scene meant that neither pixel- or object-based classification could be consistent. With eelgrass overlapping algae in Valino Island, the spatial detail parameters in OBIA and cluster merge parameters in unsupervised classification were different from those for Collver Point. Moreso, the small coverage of eelgrass at both sites, along with overlapping spectral characteristics between vegetation, resulted in vast overestimation of eelgrass that would need to be manually re-digitized for higher accuracy. Compared to previous eelgrass UAV mapping using RGB imagery, the low coverage of eelgrass in South Slough revealed that both pixel- and object-based classification techniques are less suitable for declining eelgrass beds in complex tidal marshes at low tide. Acquisition of a multispectral sensor on the UAV platform in future mapping attempts has potential to set the foundation for a repeat mapping/monitoring routine with the benefits of high resolution imagery, low cost for repeat surveys, and flexibility for achieving optimal environmental conditions. Alternatively, by-hand

classification of eelgrass is an even lower cost option for eelgrass monitoring that is more common than automated classification (Hossain et al. 2015). This alternative is explored in Chapter 4.

CHAPTER III

MAPPING EELGRASS WITH NATIONAL AGRICULTURE IMAGERY PROGRAM (NAIP) IMAGERY

Introduction

Prior to the introduction of UAVs for spatial ecology and conservation GIS, remote sensing served these fields through high spatial resolution aerial and satellite imagery. The 21st century welcomed a fleet of new and largely commercial satellite sensors that provide data at higher spatial and temporal resolutions than previous satellites: Quickbird, IKONOS, GeoEye-1, OrbView-3, WorldView-2, and others. Loarie at al. (2007) described three operational constraints that limit such data for ecological studies: (1) cloud contamination within scenes can obscure features of interest; (2) suitable repeat times frequently require oblique view angles that distort geometric and radiometric pixel properties; and (3) there is a high cost per scene. Moderate spatial resolution (MSR) satellites, which can be less expensive and have similar temporal resolutions, are capable of studying seagrass spatial distribution (Ferguson et al. 1997, Ward et al. 2003), but are biased towards seagrass meadows that are large, free from species intermingling, and not fragmented (Dekker et al. 2006). Although the most popular MSR satellite, Landsat, has been widely successful in mapping seagrass, it has been limiting in mapping low seagrass coverage areas (Dekker, Brando, and Anstee 2005, Wicaksono and Hafizt 2013). Given the continuous decline in global seagrass coverage, conservationists must create affordable, long-term monitoring plans with

reliable imagery sources of higher spatial resolution. Various statewide or nationwide imagery initiatives may aid in these efforts.

The National Agriculture Imagery Program (NAIP) is an effort created by the USDA Farm Service Agency's Aerial Photography Field office that collects imagery across the continental USA. With a three-year cycle, the 3-4 band orthophotography is gathered during the agricultural growing seasons and is typically provided free of cost to both the public and governmental agencies within a year. The consistency of quality, the 1m spatial resolution, and the accessibility of NAIP imagery makes it a strong candidate for species distribution mapping, such as eelgrass. Since the program began in 2003, NAIP imagery has been dominantly utilized as an aid for georectifying other aerial imagery for eelgrass mapping (Tiner at al. 2010, CDFW 2016). Additionally, 2005 NAIP imagery had a 91% overall accuracy in classifying 2200 hectares of suitable eelgrass habitat in a 2008 project in Humboldt Bay, California (Gilkerson 2008).

In South Slough, Oregon, eelgrass in the extent of the entire estuary has been mapped with aerial imagery in 2005 and 2016 through proprietary vendors. The imaging sensors onboard civilian aircraft platforms are competitive for their fine-scale capabilities and fast acquisition times. Nonetheless, singular, infrequent attempts to document the spatial distribution of eelgrass for delineating habitat boundaries are inadequate, given that interannual variations in eelgrass cover are common (Gilkerson 2008, Fonseca et al. 1998). Thus, one-time expenditures to contract a vendor for imagery can be inefficient unless future plans are developed for further image acquisition (Anderson and Gaston 2013). NAIP imagery directly addresses issues with other airborne imagery sources, by implementing quality control rules on the amount of cloud contamination allowed and

being freely available to the public on a three-year cycle. Understanding the role that NAIP and other imagery providers can play in eelgrass conservation is vital for slowing its rapid decline and gaining knowledge on suitable habitat. This research explores the applicability of NAIP imagery towards repeat eelgrass mapping in South Slough by investigating the accuracy of 2016 RGB imagery in classifying eelgrass at two sites within South Slough. Different classification techniques (unsupervised versus supervised, pixel- versus object-based) in order to compare the effectiveness of different classification approaches.

Dataset

On June 16, 2016, NAIP acquired imagery of Coos estuary at a spatial resolution of 1m. Digital sensors captured the scene with no more than 10% cloud cover per quarter quad tile at a height of 8400m above ground level. The 4 final corrected products that contained South Slough were stitched together to render an orthomosaic for this study.

An eelgrass map produced by Quantum Spatial, Inc. (QSI) in 2016 was used as a reference for training samples and validation points in the classifier training and accuracy assessment of these clipped orthophotos. The 25cm spatial resolution imagery was contracted through Quantum Spatial, Inc. (QSI) by the Friends of the South Slough (FOSS) in 2016. QSI collected orthoimagery of the Coos Estuary study area on July 6, 2016 during low tide conditions with a sun angle >30 degrees “in order to receive ideal image contrast and eelgrass visibility” (Yednock & QSI Corvallis 2017). Positional coordinates were gathered onboard using a differential GPS unit, while two ground survey monuments in the flight path were referenced to support spatial accuracy. 321

images were gathered with 80% overlap along track and 60% sidelap between frames and eelgrass was classified in areas where single beam sonar transect data from David Evans and Associates (DEA) identified eelgrass (Yednock & QSI Corvallis 2017). The in situ data referenced for the original mapping consisted of monitoring data from SSNERR as well as the DEA sonar data. The final QSI map separates eelgrass classes into five confidence classes (Table 4).

Table 4. Confidence classes for the eelgrass map created by QSI in 2017. Reprinted from "Coos Estuary, Oregon Orthophotography and Eel Grass Feature Extraction Technical Data Report – Revised" by Yednock, B. & QSI Corvallis. (2017).

Category	Confidence	Description
5	High	Hand digitized eelgrass beds
4-3	High-Medium	Spectrally and contextually positive for eelgrass
2	Low	Spectrally or contextually positive for eelgrass, but otherwise questionable
0/NA	NA	Did not register positive for eelgrass

The orthophoto was clipped to the extent of the three study sites formulated for UAV mapping in 2019 (Figure 4). I projected the QSI map into NAD-83 UTM Zone 10 in order to match the projections of the NAIP imagery and for more accurate spatial geometry analysis (Chapter 4).

Classification

The classification scheme for the 2016 NAIP imagery remained consistent with the classification scheme applied to the 2019 UAV imagery. For eelgrass sites, the scheme consisted of eelgrass, algae, substrate, and water. For non-eelgrass, the eelgrass

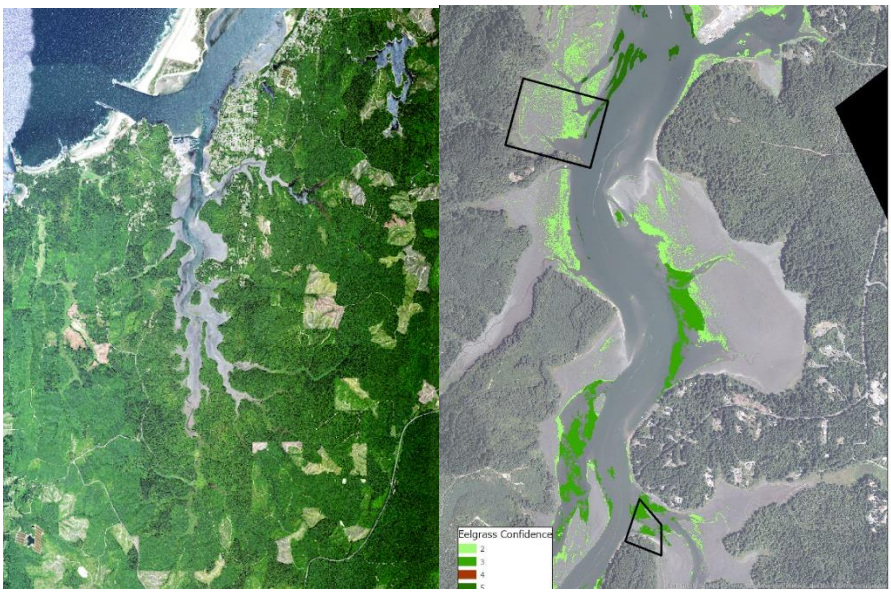

Figure 4. The June 2016 NAIP orthophoto (left) and July 2016 eelgrass map from QSI (right) with the QSI imagery as a basemap. Black polygons outline the two eelgrass sites. The legend refers to the confidence levels from Table 4.

class was replaced with a riparian vegetation class. The classification techniques utilized were iso cluster unsupervised classification, support vector machine (SVM) supervised classification, and object-based SVM classification (OBIA). Discrepancies between these classifiers was discussed in Chapter 2. Training samples for supervised classification had ~50 pixels per class. The parameters set for iso cluster training and image segmentation differed in both imagery sets from 2019 analysis due to differences in spatial distribution and continuity of aquatic vegetation. Specifically, merge distances in the iso cluster unsupervised classification were reduced from 5 to 3 and the spatial detail parameter in OBIA segmentation was decreased to values of 10 and 13 for Valino Island and Hidden Creek to prevent the classifier from perceiving continuous eelgrass or algae patches as separate objects.

A stratified random sampling design was applied to both pixel- and object-based classifications within ArcGIS Pro. I assessed the accuracy of the three classifiers by

comparing the reported eelgrass coverage of 80 randomly selected points to the real-life eelgrass. Training samples and validation points were derived from the June and July 2016 monitoring data done by SSNERR and the sonar-validated eelgrass classification from DEA and QSI. Only confidence levels of three and above were used to validate accuracy of the classifications.

The effectiveness of the aerial imagery for mapping eelgrass was determined by the classification accuracies. A confusion matrix was calculated for each study site and each classification technique, resulting in three confusion matrices for each site and each dataset. The assessment of effectiveness of the aerial imagery only included the user's and producer's accuracies because the overall accuracy and Kappa statistic incorporate the accuracies of other classes in the classification scheme, which are not relevant to the purpose of this study. Errors of commission/Type I error (measured as 1 – user's accuracy %) and omission/Type II error (measured as 1 – producer's accuracy %) are used interchangeably to communicate results.

Results

The individual accuracy assessments for each study site and classification technique are

compared in Table 5, while the classified maps can be viewed in Figure 5. Overall, SVM supervised classification performed best at two of three sites, with OBIA classification ranking second. Interpretation of classification results specific to each site are listed afterwards.

Table 5. Accuracy results for eelgrass at each site and algae at the control site. Shaded gray cells indicate the most effective classification technique for eelgrass/algae at each site.

Site - Class	Classification technique	Producer's accuracy	User's accuracy	Average site accuracy (P/U)
Valino Island - Eelgrass	Iso cluster unsupervised	71%	50%	63/70
	SVM supervised	45%	100%	
	Object-based SVM	75%	60%	
Collver Point - Eelgrass	Iso cluster unsupervised	33%	10%	66/27
	SVM supervised	100%	50%	
	Object-based SVM	66%	20%	
Hidden Creek - Algae	Iso cluster unsupervised	85.7%	60%	95/50
	SVM supervised	100%	30%	
	Object-based SVM	100%	60%	

Hidden Creek

Hidden Creek was included as a study site in order to explore how accurately 1m spatial resolution aerial imagery could map estuarine aquatic vegetation within tidal marshes when algae is not mixed with eelgrass. The site was imaged at low tide and water was found predominantly in the inundations of the tidal banks close to shore. Microalgae cover was extremely low and potentially underestimated due to spatial resolution and sun glint during image acquisition. However, the NAIP imagery displayed errors of commission more so than errors of omission, with probabilities of 40-70% that the algae classified did not exist in such locations (Table 5). Microalgae was typically misperceived in wet substrate and along the transition zone between salt marsh and mudflat.

OBIA resulted in the highest user's and producer's accuracies for algae classification, notably not misclassifying the riparian banks as algae (Table 5). However visual photo interpretation showed that both unsupervised iso cluster and supervised SVM forms of pixel-based classification portrayed more realistic results than OBIA, in which algae is less clumped, more fragmented, and less prevalent close to shore.

Valino Island

Unlike Hidden Creek, the Valino Island scene had both issues of commission and omission. Tidal heights submerged all eelgrass and algae. Ripples in the water surface were prevalent in both scenes, while unideal sun angles obscured the water column with glint in the tidal channel (Figure 5). Spectral mixing due to vegetation submersion caused eelgrass to be both misidentified as algae and wrongly omitted for water.

Accuracy assessment reported that supervised pixel-based (SVM supervised) classification was most accurate of the three techniques for the scene. Visual inspection showed that unsupervised classification rendered the most accurate geometries of eelgrass beds compared to salt-and-pepper pattern of algae and eelgrass in the two supervised classifications (Figure 5).

Collver Point

June and July scenes show low tidal heights with low turbidity in the water column, which allowed for high producer's accuracy in pixel- and object-based supervised classifications. Unsupervised classification falsely tested positive for eelgrass in the

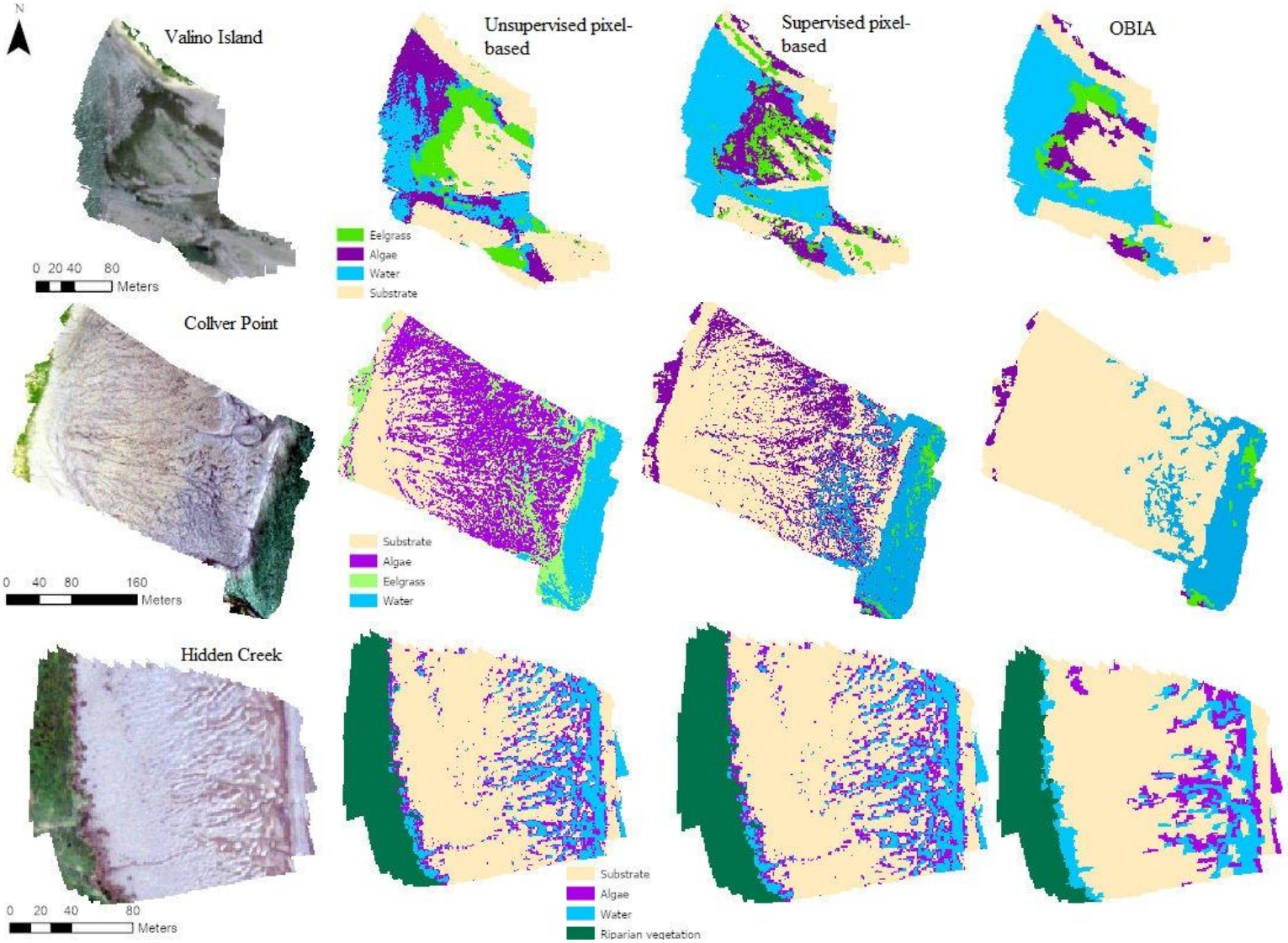

Figure 5. 2016 NAIP RGB orthophotos and classification results for Valino Island, Collver Point, and Hidden Creek.

inundated portions of the shoreline, while supervised classifications accurately differentiated algae and eelgrass with no manual digitization required. Errors of commission were exaggerated in user's accuracy results, as the only areas where eelgrass was wrongly overestimated were at the shoreline in the southeastern corner of the scene. The low coverage of eelgrass at the site may exacerbate the few Type I and II errors present to present mixed results, yet the OBIA classification was highly accurate upon visual inspection.

Discussion

Visual inspection of classified maps to the 2016 QSI maps showed that OBIA performed best at Valino Island, while iso cluster unsupervised classification identified eelgrass best at Collver Point. The clustering performed in the iso cluster classifier could have reduced the salt-and-pepper effect found in the SVM supervised classification. Unsupervised classification also outperformed SVM classifiers in supervised classification of eelgrass at spatial resolutions of 0.4cm (Duffy et al. 2018). Additionally, low spectral variation in algae and eelgrass training samples could have amplified the number of false negatives produced. Contrastingly, the minimal differences between unsupervised and supervised pixel classification at Hidden Creek suggest that classes were spectrally separable enough to be delineated without training samples.

Although the classifier performances between 2016 NAIP (1m) and 2019 UAV (25cm) imagery cannot be directly compared due to differences in eelgrass coverage, the studies suggest that tidal conditions and habitat complexity are as important as image resolution. High spatial resolution imagery can decrease accuracy due to amplifications

of sunglint, sensor noise, light attenuation, and intra-habitat variation due to tidal fluctuation (Hossain et al. 2015). In 2019, the highest producer's and user's accuracies (%) for Valino Island and Collver Point were 100/20, whereas accuracies in this study were 75/60 and 100/50. Major differences in scene conditions were: tidal height, proximity of algae to eelgrass, and spectral variation in eelgrass. Higher tidal heights and different eelgrass placements in 2016 meant that the large within-species spectral variability in eelgrass was not present as it was in 2019 due to the presence of both exposed and submerged eelgrass, which resulted in high user error.

The accuracy rates may have been higher if imaging had occurred at more ideal eelgrass mapping conditions, such as lower sun angles and wind speeds (Nahirnick et al. 2018). The fixed frequency of NAIP imagery has a downside; the lower flexibility in timing of image acquisition can make eelgrass mapping in some years infeasible due to sunglint or tidal height. The influence of other less obvious scene conditions can be obscure, which can decrease objectivity and increase uncertainty in the accuracy assessment, especially with minimal in situ data. Metrics for testing the reliability of aerial imagery in benthic habitat mapping have been developed for analyzing imagery that may lack in situ data (Pasqualini et al. 1997, Nahirnick et al. 2018), yet the need for bathymetric data eliminates the possibility of using the reliability index for South Slough currently.

The approach to classification and accuracy assessment in this study served to most objectively evaluate various traditional classification techniques for NAIP imagery. Despite advancements in species classification methods (e.g. OBIA), classifying seagrass habitats by manual delineation was the most used method in a 2015 review (Hossain et al.

2015). Manual object-based classification has aided in classifying seagrass where inconsistent radiometric properties were present, such as cloud reflectance and changes in sun angle (Nahirnick et al. 2018, Lathrop et al. 2006). A 2017 comparison of automated classification and manual digitization concluded that automated classification had no advantages when using high resolution (0.5m) 4 band imagery due to the fine-scale differences in spectral responses of eelgrass and other submerged aquatic vegetation (SAV) (Davenport et al. 2017). Both techniques had 73% accuracy, yet low to medium density eelgrass was removed from the overall comparison because of high producer error (Davenport et al. 2017). Although the large footprint of NAIP imagery reduces radiometric differences, the increased spatial complexity of eelgrass as of 2019 in South Slough provides an opportunity for manual digitization of eelgrass in NAIP imagery to be tested for viability in more fragmented environments.

Accuracy of eelgrass classification with NAIP imagery in South Slough has been comparable to other seagrass mapping efforts. Species presence, biomass, and cover was mapped in high spatial resolution satellite data with 68-83% accuracy in similarly shallow and clear water in Moreton Bay, Australia (Hossain et al. 2015). Other high spatial resolution satellite imagery has had mixed success: 22.69% and 28.11% accuracy mapping eight classes with QuickBird and CASI in 2008; 65%+ accuracy with QuickBird, WorldView2, and IKONOS in 2014 (Hossain et al. 2015).

NAIP imagery of 1m resolution can be as effective as higher spatial resolution imagery only given that there is ancillary data. The 1m imagery renders important time series analysis difficult due to the low distinction between eelgrass and other SAV at such resolution. NAIP imagery only is acquired every three years, in which a drastic decline in

eelgrass cover can occur. However, a three-year cycle for estuary-wide eelgrass monitoring is more proactive than the absence of estuary-wide monitoring or the 11-year difference between estuary-wide eelgrass analysis in South Slough (2005-2016). Moreover, the findings of these results are still applicable towards more frequent imagery sources of 1m or less.

Although the focus of this analysis was testing performance of NAIP imagery, it is appropriate to also address the effectiveness of airborne remote sensing itself for eelgrass mapping. The time and resources required to gather and analyze eelgrass images can be unappealing when coastal organizations already have feasible in-situ monitoring practices in place. Seemingly efficient monitoring innovations via remote sensing may not be as efficient when applied to the entire spatial extent of the managed region, as remote sensing scientists often test their methods in a small percentage of the actual area of interest, as was done in this study (Andrefouet 2008). Even at relatively high spatial resolutions, ground sampling may still be necessary depending on the reliability index; high-confidence interpretation of mixed-SAV tidal marshes was not possible from 1m NAIP imagery without ground data from quadrat sampling and sonar imaging. As high spatiotemporal resolution orbital sensors (e.g. the sub-meter SkySat from Planet Labs) become more widely available, more frequent mappings of eelgrass will become possible with more spectral bands, which could eliminate accuracy concerns expressed here. Furthermore, the scientific knowledge gained from incorporating further spatial analysis (rather than simple presence/absence species distribution mapping) on gathered imagery may outweigh the costs of acquiring and classifying estuary-wide imagery. The utility of aerial image time series for spatial ecology is explored in the next chapter.

CHAPTER IV

EELGRASS CHANGE IN SOUTH SLOUGH, 2016-2019

Introduction

Eelgrass (*Zostera marina*) is a marine keystone species found in the coastal regions of North America and Eurasia that provides one of the most productive ecosystems on the planet, matched with those of corn and sugar cane (McRoy and McMillan 1977). The species provides safe habitat for Pacific salmon (*Oncoryhnchus spp.)* following their journey to the coast, as well as provides ecosystem services to commercial fisheries worth up to $3500 per hectare per year (Watson Coles and Lee 1993). Eelgrass participates in the sequestration of "blue carbon", sediment stabilization, and water quality enhancement (Waycott et al. 2009).

Various factors play into the spatial distribution of eelgrass landscapes (Phillips 1984). The landscape in intertidal and subtidal areas can range from fragmented, small, and sparse patches to dense and large meadows (Phillips 1984). Water depth plays a role in how and where eelgrass is displayed: the vegetation is limited by desiccation and photosynthesis from 1.8m above mean lower-low water (MLLW) to 6.6 m below MLLW, given that the water is clear (Phillips 1984). Wave energy also influences eelgrass patterns, with sheltered areas allowing for large continuous meadows and exposed areas portraying more fragmented and complex patches (Frederiksen et al. 2004).

Water quality degradation and stronger coastal storms have put increased stress on eelgrass, which is contributing to the global decline in seagrass ecosystems (Waycott et al. 2009). Eelgrass and other seagrasses have been estimated to be lost at a rate of 5%

per year collectively, with a total loss of 29% since the late 19th century (Waycott et al. 2009). Other natural disturbances documented as drivers of local and regional declines include eelgrass "wasting disease" and bioturbation by stingrays and turtles (Uhrin and Turner 2018, Christiansen 2014). The most dominant drivers of the decline worldwide are anthropogenic disturbances: coastal development, nutrient loading in the watershed, dredging, and introduction of invasive species (Short and Wyllie-Echeverria 1996). Timely research, conservation, and restoration of the genus is crucial for the future of eelgrass and the organisms and abiotic processes that depend on it.

Monitoring and conservation of current eelgrass populations is even more important given that restoration has low success rates with high costs. With no national or international standard on eelgrass restoration and suggested research guidelines being only loosely followed, it is not possible to quantitatively compare restoration successes with confidence (Thom et al. 2008). However, Stamey (2004) calculated that only 13% of Pacific Northwest projects were successful in all metrics. In a 2008 gathering of Pacific Northwestern researchers and practitioners, the coalition reported that "the question remains whether eelgrass can be reliably restored" despite over half of a century of eelgrass and seagrass experience (Thom et al. 2008). Cunha et al. (2012) argued that the majority of “successful” seagrass restoration projects in Europe are biased in that their monitoring period was less than one year, obscuring the severity of restoration failures in the region. Even though early problems with suitable site identification have been solved, eelgrass restoration has not prevented a net loss of eelgrass habitat (Fonseca et al. 1988).

High spatial resolution imagery has been used for temporal change detection and monitoring declines of eelgrass spatial distribution, as well as measuring success of

eelgrass restoration (Ferguson et al. 1993, Bulthuis 1995, Ward et al. 2003, Dekker et al. 2005, Costello and Kenworthy 2009). Mapping intertidal aquatic vegetation with high resolution airborne imagery at low tide has been performed successfully and data acquisition is relatively inexpensive at large scales (Ferguson et al. 1993, Krause-Jensen et al. 2004). The efficiency of these methods at mapping large eelgrass landscapes encourages their use within eelgrass research. Furthermore, continuous mapping of eelgrass decreases the likelihood that changes in spatial distribution are occurring undetected, a constant risk implicit in field-based methods that rely on sampling to represent the status of the overall seascape.

Ecologists value high resolution aerial imagery not only for its temporal change detection at large scales but its ability to measure spatial metrics at higher densities and frequencies than possible on the ground. Aspects of seagrass landscapes, such as their formation of mosaics and their distributions in shallow waters that allow for analysis by airborne imagery, are analogous to terrestrial ecology and thus permit for adoption of airborne techniques used in terrestrial landscape ecology (Robbins and Bell 1994, McGarigal 1995). Patch dynamics such as the number of patches, patch shape, and leaf area index have been monitored using high resolution satellites, multispectral and hyperspectral airborne sensors, and recently, UAV technology (Fyfe 2003, Lyons et al. 2015, O'Neill et al. 2013, Frederiksen et al. 2004, Barrell and Grant 2015, Ventura et al. 2016, Duffy et al. 2018).

In a time of widespread eelgrass loss, the incorporation of spatial ecology metrics into traditional eelgrass change detection benefits our knowledge of the relationship between spatial characteristics and system resiliency. Recent research has suggested that

complex and fragmented patch shapes are more susceptible to negative effects of poor environmental conditions and could indicate critical transitions in the landscape state (Carr et al. 2010, Uhrin and Turner 2018). In 2007, van der Heide et al. attempted to explain the loss and lack of recovery of eelgrass beds in the Dutch Wadden Sea in the early 20th century using the theory of alternative stable states. With the positive feedback system between seagrass, substrate, and light availability, seagrass ecosystems were suggested to have an alternative stable state which was enabled once a change in conditions (such as increasing turbidity) initiates decrease in resilience from seagrass and collapse into the alternative stable state of bare sediment. Measured wave orbital velocity in the latter 20th century supported the theory, as velocity was consistently too high to allow for a reversal of the bare sediment state to eelgrass habitat (van der Heide et al. 2007). Identification of early warning indicators (EWIs) in eelgrass systems and implementation of such variables into monitoring efforts could reduce eelgrass loss on a global scale.

One of Oregon's major estuaries, Coos Bay, is a target for eelgrass research (Borde et al. 2003, Thom et al. 2005, Rumrill and Sowers 2008). The South Slough National Estuarine Research Reserve (SSNERR) has been monitoring eelgrass at three sites in South Slough (Collver Point, Valino Island, and Danger Point) annually since 2004 for the NERRS Biomonitoring Pilot project to test protocols and document spatial distribution and seasonal dynamics of eelgrass (Moore 2009) and quarterly at Valino Island as part of the SeagrassNet program (Short et al. 2015). SSNERR added Hidden Creek to the monitoring list in 2010 for the NERRS Sentinel Site Biomonitoring program (Moore 2017). Before 2016, eleven years of monitoring at Valino Island, four years of

monitoring at Collver Point and Danger Point (2004, 2005, 2010, 2016), and six years of monitoring at Hidden Creek showed relatively stable average percent cover and shoot density. Beginning in 2016, eelgrass cover and density decreased at Valino Island, Collver Point, and Hidden Creek, exposing bare mudflats and sparse patches of eelgrass at Valino Island. Similar declines began at Danger Point in 2018 and complete absence of eelgrass at Danger Point and Hidden Creek continued into 2019 (Wirfs and Helms, 2018). No similar trends have been observed in other parts of Coos Bay monitored by two Oregon State University (OSU) collaborative research projects (OSU Sea Grant, Tomas-Nash 2015-17; OSU/OA, Magel, Chan, and Hacker 2016-18) and the Oregon Department of Fish and Wildlife Shellfish and Estuarine Assessment of Coastal Oregon (ODFW SEACOR, D'Andrea 2017).

This research uses high spatial resolution aerial imagery to evaluate changes in eelgrass spatial distribution at two sites in South Slough between 2016 and 2019. The time lapse between scenes in this research is relatively short compared to other eelgrass change studies (Fredericksen et al. 2004, Ward et al. 2003, Nahirnick et al. 2018). Significant changes in areal coverage were found in intervals of seven years between photos (Frederiksen et al. 2003); however, change detection of short time periods can be important when an area has recently been disturbed or restored (Davenport et al. 2017). Traditional change detection at Valino Island and Collver Point is applied via image classification and overlay. Seven landscape metrics (percentage of landscape, number of patches, mean patch area, largest and smallest patch area, area, perimeter, and shape index) are calculated to assess changes in patch dynamics. The results can contribute to

the decision-making process of SSNERR in creating a subsequent eelgrass conservation plan post-2019.

Imagery and Classification

The imagery used for the analysis of spatial eelgrass distribution from 2016-2019 consisted of QSI aerial imagery from July 2016 and UAV imagery taken for this study from July 2019. Both have spatial resolutions of 25cm. The orthophoto of Coos Bay in July 2016 was clipped to the orthophotos from the UAV flights in 2019. Training and validation samples were derived from quadrat monitoring data collected prior to each flight. ISO cluster unsupervised classification, support vector machine (SVM) supervised classification, and object-based SVM supervised classification was tested on imagery in order to find the most accurate method of remote eelgrass identification. Chapter 2 describes accuracy assessment of 2019 imagery, while the process of identifying the best classifier for 2016 imagery is described here. Details of the imagery collection and vegetation classification can be found in Chapter 2 (2019) and 3 (2016). For the purpose of this research, some eelgrass segments that were originally omitted during classification were manually digitized using the Reclassifier tool from the ArcGIS Pro Image Classification toolbox to reduce errors in the change detection.

Change Analysis

Land cover classes were converted into vector polygons to calculate areal coverage in square meters. Net change in eelgrass coverage was reported in square meters, while an index of relative change was employed to quantify the change in spatial

distribution regardless of the direction of the change. The index adopted from Fredericksen et al. 2004 is:

$$index\ of\ relative\ change = \frac{loss + gain}{loss + gain + common}$$

Common refers to the area (m^2) of eelgrass that remained in the same position from 2016 to 2019. An index of 0 means no change occurred, while an index of 1 means all eelgrass had changed. An ArcGIS Union operation was performed to visually represent areas of eelgrass gain, loss, and no change.

Patch Geometry

Four class-level landscape metrics (percentage of landscape, number of patches, mean patch area, largest and smallest patch area) and three patch-level landscape metrics (patch area, perimeter, and shape index) were generated to characterize the distribution and composition of the eelgrass at each site. I calculated the shape index (SI) of the eelgrass patches in order to measure the complexity of the eelgrass patch shape. The SI compares the patch shape to a standard square of the same area, which resolves the size dependency issue present in the perimeter-area ratio: an increase in the size of a constant shape will decrease the ratio (Forman and Godron 1986). The equation is as follows:

$$S = \frac{0.25P}{\sqrt{A}}$$

where P represents the perimeter and A is the area. A standard square has a SI of 1, and the dimensionless index increases as the shape becomes more complex. There is no upper limit to the index.

Results

2016

Classification accuracy of eelgrass delineation in 2016 showed that no classification technique was consistently best at more than one site (Table 6). Pixel- and object-based classification outperformed the classifiers in the 2019 imagery (see Chapter 2), which may be due to multiple factors. Similar to 2019, OBIA performed best at Collver Point, with pixel-based classification performing best at Valino Island. Spectral similarities between riparian vegetation, algae, and eelgrass prevented an error-free automation of eelgrass delineation, so I manually digitized eelgrass patches that were unclassified using a freehand selection tool and changed the class type of algae that had been misclassified as eelgrass. Manual digitization of eelgrass is the most common way to map eelgrass (Hossain et al. 2015). The OBIA-rendered map was ultimately chosen as the map to detect change in eelgrass due to its relative success and ease in manually editing and creating eelgrass polygons (Figure 6).

Table 6. Accuracy assessment results of different classification techniques for eelgrass in 2016 QSI imagery. No classification technique was consistently best across sites.

Site - Class	Classification technique	Producer's accuracy	User's accuracy	Average site accuracy (P/U)
Valino Island - Eelgrass	Iso cluster unsupervised	88%	80%	75/80
	SVM supervised	62.5%	100%	
	Object-based SVM	75%	60%	
Collver Point - Eelgrass	Iso cluster unsupervised	0%	00%	67/37
	SVM supervised	100%	50%	
	Object-based SVM	100%	60%	

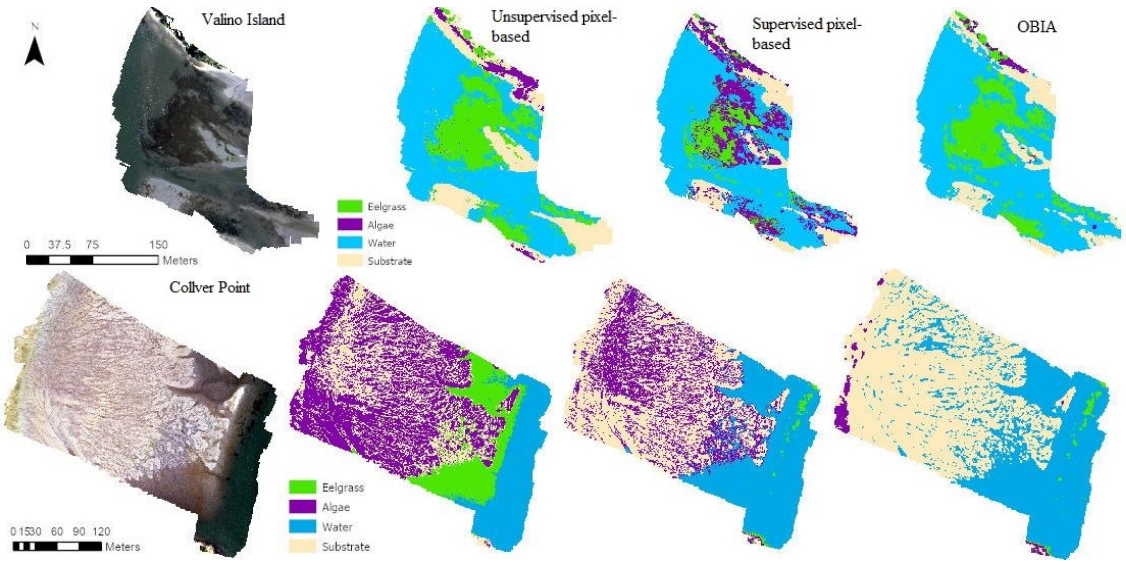

Figure 6. 2016 QSI RGB orthophotos and classification results.

In 2016, eelgrass was found in the sandflats and along the fringe of the tidal channel at Valino Island (Figure 7). Eelgrass coverage was 6994m^2, totaling 21.4% of the site. The landscape metrics are listed in Table 6. The SI, as well as other spatial landscape metrics, are affected by the scale of the analysis. When the area of the patch nears the resolution of the mapped eelgrass, the indices universally approach 1 (Figure 8). Due to the small sample of patches in the study, no patches were excluded from the analysis.

Eelgrass was only present along the tidal channel at Collver Point (Figure 7). As 2016 imagery was scaled to 2019 imagery, the site size was much larger than the area of eelgrass (Table 7). Patch complexity was low and comparable to that of Valino Island, with an average SI of 1.9.

2019

Eelgrass at Valino Island in 2019 was estimated to be 10.5% of the total site, showing a loss in half of the previous distribution. The patch- and class-level metrics

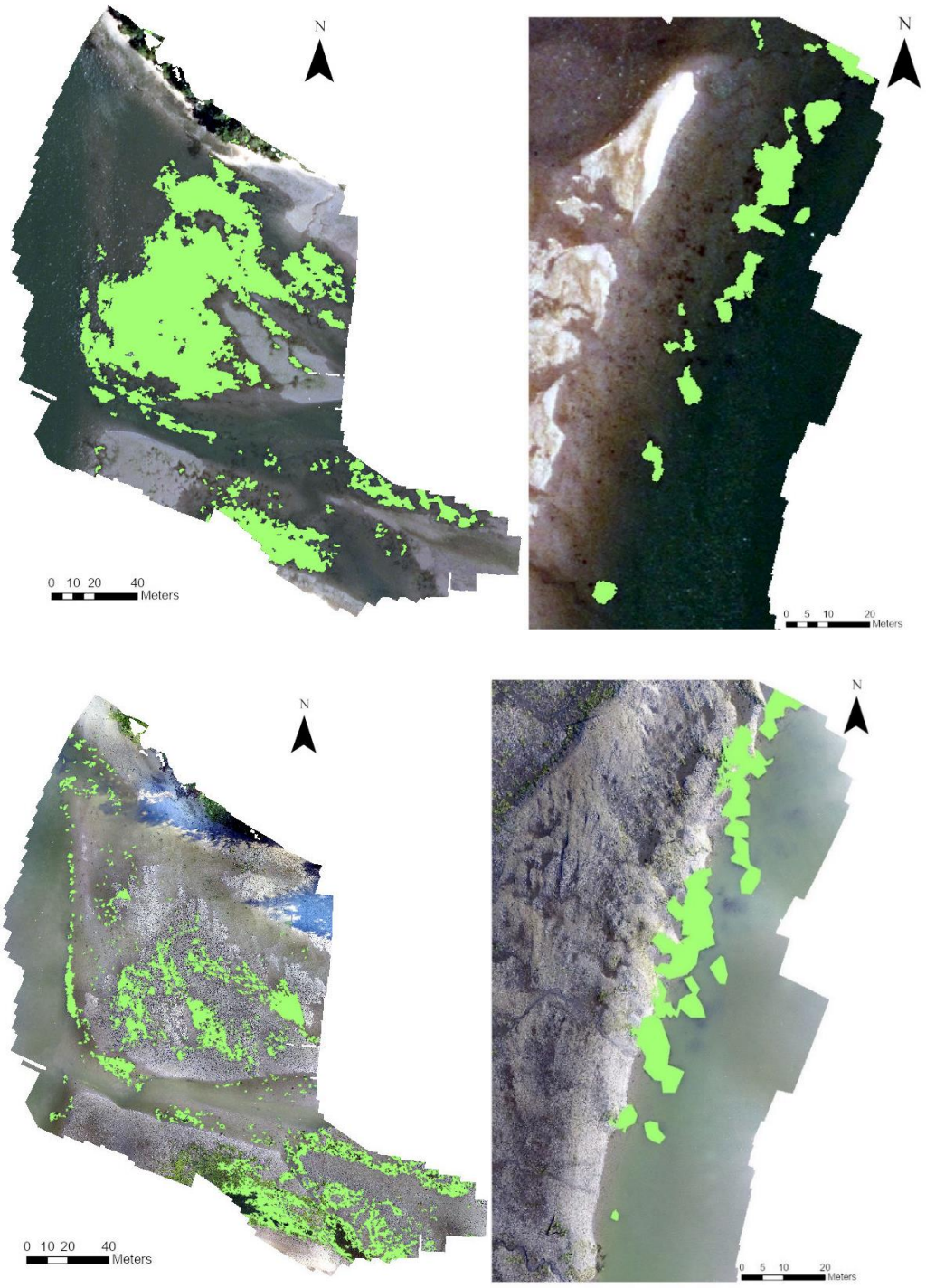

Figure 7. Valino Island (left) and Collver Point (right) eelgrass distribution in July 2016 (top) and July and August 2019 (bottom), represented by green polygons.

reflect decreases in average size and increases in fragmentation and shape complexity (Table 7).

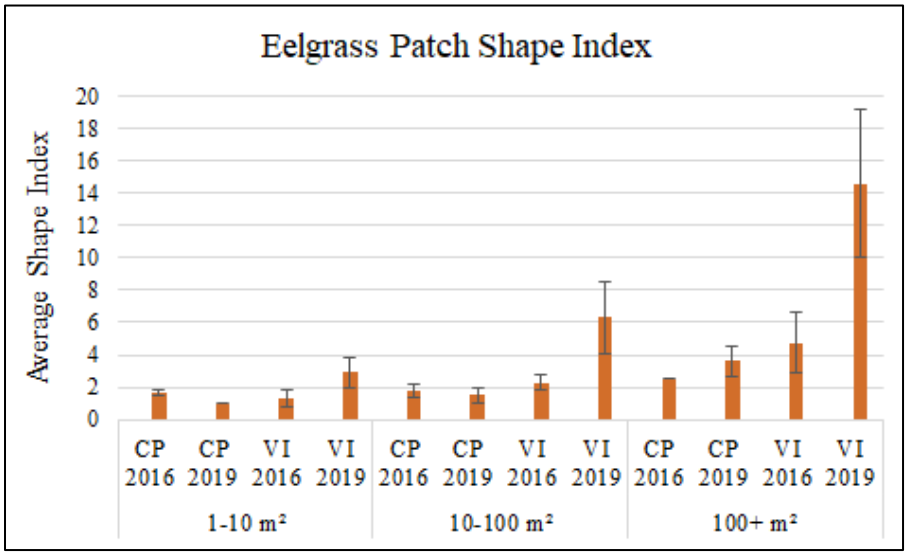

Figure 8. Average shape indices at Collver Point (CP) and Valino Island (VI). The horizontal axis is categorized by patch area classes. Shape complexity increases as the shape index increases. A shape index of 1 is for simple forms (i.e. a square). Mean values ± SD.

Table 7. Spatial landscape metrics for eelgrass at Valino Island and Collver Point in 2016 and 2019.

Year	Site	Area (m^2)	Percentage of landscape	Patches	Minimum patch size (m^2)	Maximum patch size (m^2)	Average patch size (m^2)	Average shape index
2016	Valino Island	6994	21.4%	99	0.5	5327	70	1.6
	Collver Point	463	0.63%	14	2	172	33	1.9
2019	Valino Island	3430	10.5%	537	0.5	453	30	3.3
	Collver Point	682	0.89%	8	3	203	85	2.2

Collver Point experienced new eelgrass growth in 2019. Patches continued to inhabit the edge of the tidal channel with an elongated geometry. The total area increased from 0.63% to 0.89% of the site, and all spatial metrics had positive change (Table 7). However, complexity of the patch geometry had a small increase (Figure 8).

2016-2019 change

Overall, there was a 44.8% net loss of eelgrass (6794m^2) across the two sites in South Slough. Specifically, 50.9% of eelgrass was lost at Valino Island and a 32.2% increase occurred at Collver Point in the three-year period. Valino Island experienced loss in the higher elevations of its occurrence: namely in a large bed in the sandflats, as well as minor losses along the tidal channel and southern shore (Figure 9). However, new growth was seen in similar elevations, fringing on the tidal channel and in small fragments around the previous extent in the sandflat. The index of relative change here was 0.96 on a scale of 0 to 1, due to the small amount of eelgrass that remained across the time period (305m^2) compared to the eelgrass that died-off (6478m^2) or grew in new areas (2915m^2).

At Collver Point, there was a migration of eelgrass into lower MSL (Figure 9). Large areas of new growth portray elongated geometries similar to previous big patches. The index of relative change was 0.45.

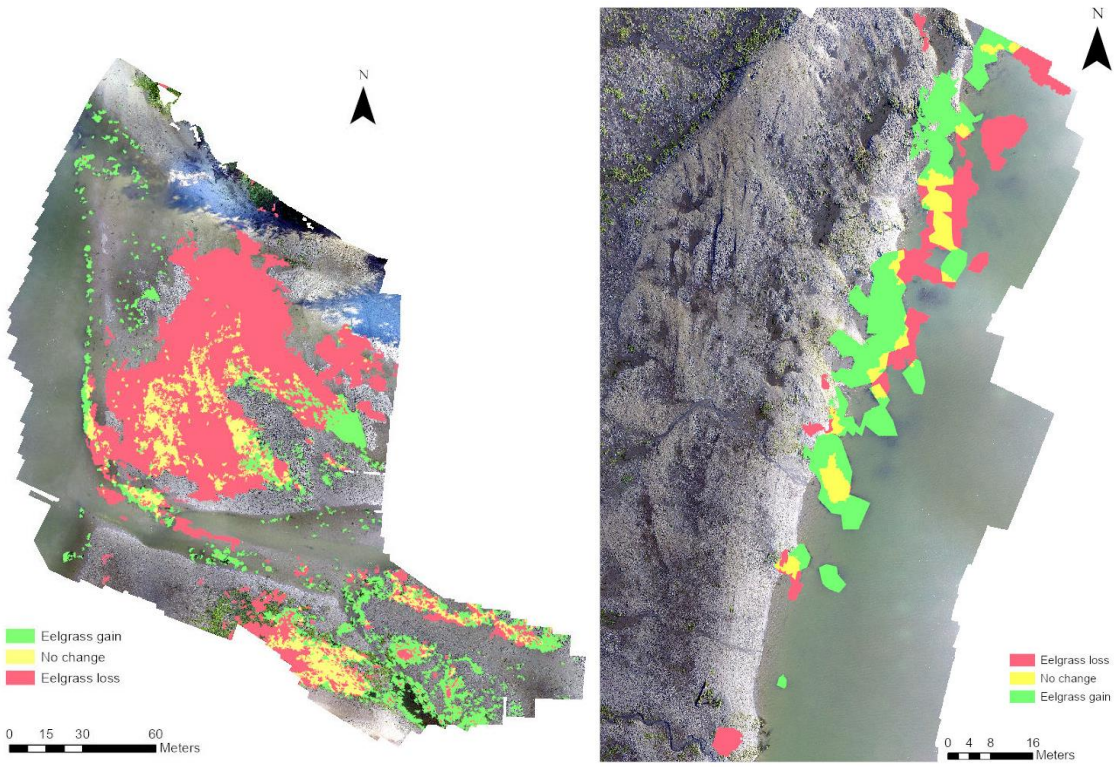

Figure 9. Eelgrass change maps for Valino Island (left) and Collver Point (right) between 2016 and 2019.

Discussion

Temporal change detection of a 3-year period at Collver Point and Valino Island revealed a loss of nearly 50% of all eelgrass habitat (~6800m^2) combined. Although only Valino Island experienced negative net change, many documented drivers of eelgrass loss act at the watershed-level, so the location of Collver Point need not be excluded from discussion of potential drivers. In the Coos estuary, there are several changes that could be affecting eelgrass habitat. First, ocean water has been warmer than the 15-year monthly average since 2014, and water temperature is increasing in the mid and upper estuary, while salinity is decreasing (Beck et al. 2018). The majority of eelgrass

worldwide inhabits sea temperatures of 5-27°C with an optimum range of 10-20°C, while salinity limits eelgrass to optimal regions of 10-30ppt (Phillips 1984). The salinity gradient in South Slough averages from 0-33 psu (Rumrill 2015). The complete loss of eelgrass in 2016 and 2018 at further upstream sites Collver Point and Danger Point support the hypotheses that increase in water temperature and/or decrease in salinity are major causes of eelgrass decline. A 2012 coupled vegetation-growth hydrodynamic model of eelgrass in Hog Island Bay, Virginia, USA demonstrated that eelgrass meadows are likely to withstand sea-level rise, yet an increase in the frequency of days where water temperature exceeds 30°C will cause more summer die-offs by limiting meadows to cooler but deeper water levels, which are outside the bistable depth range (1.6-1.8 MSL) in which eelgrass can receive sufficient light and low turbidity levels (Carr et al. 2010). However, new eelgrass growth at Collver Point between 2016 and 2019 occurred at lower MSL (Figure 9), and average subsurface temperatures in Coos Bay do not average above 11°C, suggesting colder temperatures may be a factor affecting eelgrass distribution in South Slough (Rumrill 2015).

Second, increased logging in the upper Coos watershed is increasing sediment inputs in the estuary, which can be affecting photosynthesis in the water column (Ali Helms (SSNERR) personal communication, February 2, 2019). The positive feedback system caused by seagrass, suspended sediment, and light availability can lead to critical bifurcation of the stable ecosystem state (van der Heide et al. 2007). Third, eelgrass wasting disease has been identified in the Coos estuary (Yoshioka 2019). The impact of the disease on the time period discussed here is unknown, but eelgrass wasting disease was the leading driver of the loss of 90-100% of eelgrass in the North in the 1930s

(Phillips 1984). Lastly, ulvoid macroalgae blooms have had negative effects on eelgrass density at marine and riverine locations in South Slough (Hessing-Lewis et al. 2010). Macroalgae was intermixed with eelgrass at Valino Island in August 2019, notably in locations where patch fragmentation had occurred, but was not present in Collver Point eelgrass patches in either year. While this research cannot explain change in eelgrass distribution with any certainty, these potential drivers mentioned may function as building blocks for a more advanced monitoring system at designated eelgrass sites in the slough.

All spatial metrics at Valino Island displayed a drastic decline in eelgrass ability to tolerate disturbances. The site experienced a decrease in eelgrass percent cover and average patch size and an increase in shape complexity and fragmentation. Smaller patches can lead to large-scale declines due to their sensitivity to disturbances (Olesen and Sand-Jensen 1994). Edge effects from varying patch densities cause variation in ability to reduce suspended sediment, meaning that for patches of the same shape at Valino Island, the higher ratio of eelgrass at the edge versus eelgrass inside the patch causes a higher risk of an ecosystem state change than larger patches (Carr et al. 2010). Furthermore, the sparse and complex spatial patterns may be indicators themselves that such a critical bifurcation has been met: patch size distributions of seagrass have "moderately" supported a power law relationship in which high wave energy enables a state change to highly fragmented and less resilient patches (Uhrin and Turner 2018). Classical critical systems, in which disturbance and recovery processes initiate a system-wide spatial pattern, have been suggested to show threshold behavior where small alterations in environmental factors result in rapid responses from the ecosystem

properties and quality, frequently preceding a transition of the landscape state (phase) at the threshold, or tipping point (Groffman et al. 2006). The spatial distribution of organisms becomes invariant when the ecosystem nears the threshold and in 2011, Solé discovered that the frequency distribution of cluster (patch) sizes of organisms in the landscape displays power law behavior where all patch sizes are present with no dominant size; patch size distributions that display power laws portray a linear relationship on a logarithmic scale. (Solé 2011). Because power laws have revealed critical thresholds in the vegetation patterns of many different ecosystems (Scanlon et al. 2007, Guichard et al. 2003, Kizaki and Katori 1999), the similar finding by Uhrin and Turner suggests that patch sizes of eelgrass may be indicative of an eelgrass landscape nearing the threshold of undergoing a landscape state change to bare sediment. More research is necessary as this is the first time power law distributions have been studied in seagrass systems (Uhrin and Turner 2018).

After Collver Point experienced declines in 2016 and 2018, the 32% increase in coverage in 2019 emphasizes that change detected in a certain year is not always irreversible and that spatial patterns of one year may not reflect the resiliency levels of the eelgrass ecosystem. Consistent long-term monitoring allows for average trends in spatial distribution to be differentiated from abnormal extremes (Thom et al. 2010). The lack of consistent annual monitoring at Collver Point prevents the differentiation of such thresholds. It is still worth noting that shape complexity slightly increased between 2016 and 2019, implying that patches did not become more consolidated despite the increase in patch sizes.

The lack of correlation between epifaunal diversity and eelgrass patch sizes suggest that eelgrass communities function as a network (Whippo et al. 2018), which should influence the approach taken to conserving and mapping eelgrass in protected and especially non-protected estuaries. Data on epifaunal diversity in a British Columbia metacommunity showed that species richness was constant throughout patches of varying sizes (Whippo et al. 2018, Lefcheck et al. 2016). If no alternative state of equilibrium had taken over, meadow size dynamics in eelgrass habitats were not negatively affecting biodiversity, possibly due to high connectivity and dispersal rates throughout the metacommunity (Whippo et al. 2018). As epifaunal diversity can be affected by patch characteristics of other meadows kilometers away, it is likely other intrinsic and extrinsic factors in eelgrass patches are influenced by metacommunity-scale processes. Thus, eelgrass monitoring and restoration projects should best attempt to consider the health status of all eelgrass within the estuary. Furthermore, time series analyses of eelgrass landscapes would benefit from a metacommunity perspective simply for the increase in data gathered, for exploratory research purposes.

The small spatial scale of the two monitoring sites analyzed in this research cannot be extrapolated to represent eelgrass change in South Slough as a whole, but this study serves as a proof of concept for the utility of high spatial resolution remote sensing in detecting changes in eelgrass spatial patterns at the landscape and patch-scale. It also sheds light on the true logistic ease of UAV mapping in estuaries: wind, turbidity, tidal height, and sun angles drastically limit the window for acquiring imagery, with clear and sheltered waters being favorable for high accuracy mapping. Nonetheless, high spatial resolution remote sensing allows for studying within-meadow eelgrass heterogeneity that

can be more complex than simple percent cover changes. The usage of consumer-friendly UAVs for eelgrass mapping makes this research easier than ever before and can play a significant role in identifying declines in ecosystem health. The understanding of eelgrass patch dynamics and their relation to temporal changes in spatial distribution can aid in conservation and restoration efforts of this vital aquatic seagrass.

CHAPTER V

SUMMARY AND CONCLUSIONS

The goal of this research was to test the accuracy of three traditional classification techniques on eelgrass in UAV imagery, evaluate the effectiveness of using 1m NAIP imagery for eelgrass mapping, and assess temporal change of eelgrass spatial distribution and geometry in South Slough, Oregon.

First, the classification techniques (pixel- and object-based classifiers of unsupervised and supervised forms) tested on high resolution UAV imagery revealed that effectiveness of classifiers is not consistent among sites of small scales and varying complexities in South Slough. Mixed results in OBIA performance suggest that less concern be given to pixel- versus object-based automations and more effort be applied to the imagery bandwidth and acquisition time. Specifically, similar spectral characteristics between eelgrass and other aquatic vegetation encourage the use of multispectral imagery, and comparison of 2016 and 2019 scenes in this study has shown that image acquisition at low tide can decrease accuracy if eelgrass patches are both exposed and submerged. The current classification methods described here are ready for implementation without camera updates or more rigid timing of image acquisition given that a seagrass specialist devotes time to quality control via visual inspection and manual correction of the classified imagery.

Chapter III expanded on image classification methods in Chapter II by assessing the effectiveness of 2016 NAIP imagery in mapping eelgrass. NAIP imagery is a reliable source of imagery for eelgrass mapping at 3 year-periods and monitoring data, seagrass

specialists, or aerial photo reliability indices can be used as reference data. Performances of pixel- and object-based classifiers were mixed and dependent on site location, as in Chapter II. Accuracy rates of 1m NAIP imagery rivaled the performance of higher spatial resolution UAV imagery, but the higher coverage of eelgrass in the 2016 NAIP imagery may have influenced this performance. Both overestimation and underestimation were issues present in the analysis, and combined results from UAV and NAIP imagery indicate that overestimation of eelgrass presence is the most common error in mapping eelgrass in South Slough. Without improvement of classification methods or imagery bandwidth, practitioners in areas of low eelgrass coverage and mixed aquatic vegetation may need to resort to manual digitization of eelgrass, as was done for change detection in the final imagery application of this study.

The third objective, to measure change in the eelgrass distribution of the two remaining eelgrass monitoring sites in South Slough, showed a net loss in eelgrass coverage of 44.8%. Valino Island had a cover loss of 50% between 2016 and 2019 and an index of relative change of 0.94. The within-patch fragmentation and increasing shape complexity shown by the shape indices at Valino Island suggest that disturbances are affecting both landscape and patch-level eelgrass factors. However, Collver Point diverged from recent trends with a 32% increase in eelgrass cover and aggregation of previously fragmented patches, despite undergoing net loss in 2016 and 2018. This is the first known time that spatial landscape metrics have been quantified and incorporated into change detection for eelgrass in South Slough, Oregon.

This research trialed new methods for eelgrass monitoring in the form of classification techniques and new imagery sources and measured temporal eelgrass

change in an estuary that experienced unprecedented declines in eelgrass coverage. I have shown that relatively low-cost imagery sources such as consumer-grade UAV imagery and publicly available NAIP imagery can recognize low eelgrass coverage in Pacific Northwest tidal marshes with moderate success. I have also shown that aerial imagery can advance traditional eelgrass monitoring practices by quantifying and visualizing spatial landscape metrics such as number of patches and patch shape complexity. These metrics provide insight to within-patch heterogeneity that can reveal fine-scale signs of degradation or recovery previously unattainable by traditional monitoring methods. Successful methods development for eelgrass conservation can serve as a catalyst for increasing preventative and restorative efforts taken towards this highly valuable species.

REFERENCES CITED

Anderson, K., & Gaston, K. J. (2013). Lightweight unmanned aerial vehicles will revolutionize spatial ecology. *Frontiers in Ecology and the Environment*, *11*(3), 138–146. https://doi.org/10.1890/120150

Andréfouët, S. (2008). Coral reef habitat mapping using remote sensing: A user vs producer perspective. Implications for research, management and capacity building. *Journal of Spatial Science*, *53*(1), 113–129. https://doi.org/10.1080/14498596.2008.9635140

Balsby, T. J. S., Carstensen, J., & Krause-Jensen, D. (2013). Sources of uncertainty in estimation of eelgrass depth limits. *Hydrobiologia*, *704*(1), 311–323. https://doi.org/10.1007/s10750-012-1374-8

Baldwin, D. (2019). *Monitoring Aquatic Habitat Restoration Using Multispectral High-Resolution Remote Sensing. [*Thesis, University of Oregon*]*. https://doi.org/10.1017/CBO9781107415324.004

Bargain, A., Robin, M., Méléder, V., Rosa, P., Le Menn, E., Harin, N., & Barillé, L. (2013). Seasonal spectral variation of Zostera noltii and its influence on pigment-based Vegetation Indices. *Journal of experimental marine biology and ecology*, *446*, 86-94.

Barrell, J., & Grant, J. (2015). High-resolution, low-altitude aerial photography in physical geography: A case study characterizing eelgrass (Zostera marina L.) and blue mussel (Mytilus edulis L.) landscape mosaic structure. *Progress in Physical Geography*, *39*(4), 440–459. https://doi.org/10.1177/0309133315578943

Beck, M.W, O'Brien, T.D., St. Laurent, K.A., & Cressman, K. (2018). SWMPrats: Time-series and data analysis information and tool resources for the NERRS SWMP.

Blaschke, T. (2010). ISPRS Journal of Photogrammetry and Remote Sensing Object based image analysis for remote sensing. *ISPRS Journal of Photogrammetry and Remote Sensing*, *65*(1), 2–16. https://doi.org/10.1016/j.isprsjprs.2009.06.004

Blaschke, T., Burnett, C., & Pekkarinen, A. (2004). Image segmentation methods for object-based analysis and classification. In *Remote sensing image analysis: Including the spatial domain* (pp. 211-236). Springer, Dordrecht.

Borde, A. B., Thom, R. M., Rumrill, S., & Miller, L. M. (2003). Geospatial habitat change analysis in Pacific Northwest coastal estuaries. *Estuaries*, *26*(4), 1104-1116.

Bulthuis, D. A. (1995). Distribution of seagrasses in a north Puget Sound estuary: Padilla Bay, Washington, USA. *Aquatic Botany 50*, 99-105.

California Department of Fish and Wildlife (CDFW). (2016). Eelgrass - Tomales Bay [digital map]. Retrieved from https://map.dfg.ca.gov/metadata/ds0890.html

Carr, J., D'Odorico, P., McGlathery, K., & Wiberg, P. (2010). Stability and bistability of seagrass ecosystems in shallow coastal lagoons: Role of feedbacks with sediment resuspension and light attenuation. *Journal of Geophysical Research: Biogeosciences*, *115*(3), 1–14. https://doi.org/10.1029/2009JG001103

Christianen, M. J. A., Herman, P. M. J., Bouma, T. J., Lamers, L. P. M., Van Katwijk, M. M., Van Der Heide, T., … Van De Koppel, J. (2014). Habitat collapse due to overgrazing threatens turtle conservation in marine protected areas. *Proceedings of the Royal Society B: Biological Sciences*, *281*(1777). https://doi.org/10.1098/rspb.2013.2890

Costello, C. T., & Kenworthy, W. J. (2011). Twelve-Year Mapping and Change Analysis of Eelgrass (Zostera marina) Areal Abundance in Massachusetts (USA) Identifies Statewide Declines. *Estuaries and Coasts*, *34*(2), 232–242. https://doi.org/10.1007/s12237-010-9371-5

Cunha, A. H., Marbá, N. N., van Katwijk, M. M., Pickerell, C., Henriques, M., Bernard, G., … Manent, P. (2012). Changing paradigms in seagrass restoration. *Restoration Ecology*, *20*(4), 427–430. https://doi.org/10.1111/j.1526-100X.2012.00878.x

Davenport, A. E., Davis, J. D., Woo, I., Grossman, E. E., Barham, J., Ellings, C. S., & Takekawa, J. Y. (2017). Comparing Automated Classification and Digitization Approaches to Detect Change in Eelgrass Bed Extent During Restoration of a Large River Delta. *Northwest Science*, *91*(3), 272–282. https://doi.org/10.3955/046.091.0307

Dekker, A. G., Brando, V. E., & Anstee, J. M. (2005). Retrospective seagrass change detection in a shallow coastal tidal Australian lake. *Remote Sensing of Environment*, *97*(4), 415–433. https://doi.org/10.1016/j.rse.2005.02.017

Dekker, A., Brando, V., Anstee, J., Fyfe, S., Malthus, T., & Karpouzli, E. (2006). Remote Sensing of Seagrass Ecosystems: Use of Spaceborne and Airborne Sensors. In A. W. D. Larkum, R. J. Orth, & C. M. Duarte (Eds.), *Seagrasses: Biology, Ecology, and Conservation* (pp. 347 – 359). Dordrecht, The Netherlands: Springer.

Duffy, J. P., Pratt, L., Anderson, K., Land, P. E., & Shutler, J. D. (2018). Spatial assessment of intertidal seagrass meadows using optical imaging systems and a lightweight drone. *Estuarine, Coastal and Shelf Science*. https://doi.org/10.1016/j.ecss.2017.11.001

Ferguson, R. L., & Korfmacher, K. (1997). Remote sensing and GIS analysis of seagrass meadows in North Carolina, USA. *Aquatic Botany*, *58*(3-4), 241-258.

Ferguson, R. L., Wood, L.L., & D. B. Graham, D.B. (1993). Monitoring spatial change in seagrass habitat with aerial photography. *Photogrammetric Engineering and Remote Sensing 59,* 1033-1038.

Fonseca, M., Thayer, G. W., & Kenworthy, W. J. (1988). Restoration and management of seagrass systems: a review. In *The ecology and management of wetlands* (pp. 353–368).

Forman, R. T. T., & Godron, M. (1981). Patches and Structural Components for a Landscape Ecology. *Bioscience 31(10),* 733-740.

Frederiksen, M., Krause-Jensen, D., Holmer, M., & Laursen, J. S. (2004). Spatial and temporal variation in eelgrass (Zostera marina) landscapes: Influence of physical setting. *Aquatic Botany, 78*(2), 147–165. https://doi.org/10.1016/j.aquabot.2003.10.003

Frederiksen, M., Krause-Jensen, D., Holmer, M., & Laursen, J. S. (2004). Long-term changes in area distribution of eelgrass (Zostera marina) in Danish coastal waters. *Aquatic Botany, 78(2),* 167-181.

Fyfe, S. K. (2003). Spatial and temporal variation in spectral reflectance: Are seagrass species spectrally distinct*? Limnology and Oceanography, 48*(1, part 2), 463-479.

Gamanya, R., De Maeyer, P., & De Dapper, M. (2009). Object-oriented change detection for the city of Harare, Zimbabwe. *Expert Systems with Applications, 36*(1), 571-588.

Gilkerson, W. (2008). *A spatial model of eelgrass (Zostera marina) habitat in Humboldt Bay, California*. [Thesis, Humboldt State University].

Grippa, T., Lennert, M., Beaumont, B., Vanhuysse, S., Stephenne, N., & Wolff, E. (2017). An open-source semi-automated processing chain for urban object-based classification. *Remote Sensing, 9*(4), 358.

Groffman, P. M., Baron, J. S., Blett, T., Gold, A. J., Goodman, I., Gunderson, L. H., ... & Poff, N. L. (2006). Ecological thresholds: the key to successful environmental management or an important concept with no practical application?. *Ecosystems*, *9*(1), 1-13.

Guichard, F., Halpin, P. M., Allison, G. W., Lubchenco, J., & Menge, B. A. (2003). Mussel disturbance dynamics: signatures of oceanographic forcing from local interactions. *The American Naturalist, 161*(6), 889-904.

Hessing-Lewis, M.L., Hacker, S.D., Menge, B.A., & Rumrill, S.. 2011. Context-dependent Eelgrass- Macroalgae Interactions Along an Estuarine Gradient in the Pacific Northwest, USA. *Estuaries and Coasts 34*, 1169-1181.

Hossain, M. S., Bujang, J. S., Zakaria, M. H., & Hashim, M. (2015). The application of remote sensing to seagrass ecosystems: an overview and future research prospects. *International Journal of Remote Sensing*, *36*(1), 61–114. https://doi.org/10.1080/01431161.2014.990649

Hulet, A., Roundy, B. A., Petersen, S. L., Jensen, R. R., & Bunting, S. C. (2014). Cover estimations using object-based image analysis rule sets developed across multiple scales in pinyon-juniper woodlands. *Rangeland Ecology and Management*, *67*(3), 318–327. https://doi.org/10.2111/REM-D-12-00154.1

Kavzoglu, T., & Yildiz, M. (2014). Parameter-based performance analysis of object-based image analysis using aerial and Quikbird-2 images. *ISPRS Annals of the Photogrammetry, Remote Sensing and Spatial Information Sciences*, *2*(7), 31.

Kizaki, S., & Katori, M. (1999). Analysis of canopy-gap structures of forests by Ising-Gibbs states-equilibrium and scaling property of real forests. *Journal of the Physical Society of Japan*, *68*(8), 2553-2560.

Krause-Jensen, D., Quaresma, A. L., Cunha, A. H., & Greve, T. M. (2004). How are seagrass distribution and abundance monitored. *European seagrasses: An introduction to monitoring and management*, 45-53.

Laliberte, A. S., & Rango, A. (2009). Texture and scale in object-based analysis of subdecimeter resolution unmanned aerial vehicle (UAV) imagery. *IEEE Transactions on Geoscience and Remote Sensing*, *47*(3), 1–10. https://doi.org/10.1109/TGRS.2008.2009355

Lathrop, R.G., Montesano, P., & Haag, S. (2006). A multi-scale segmentation approach to mapping seagrass habitats using airborne digital camera imagery. *Photogrammetric Engineering & Remote Sensing*, *72*(5), 665–675.

Lechner, A. M., Fletcher, A., Johansen, K., & Erskine, P. (2012). CHARACTERISING UPLAND SWAMPS USING OBJECT-BASED CLASSIFICATION METHODS and HYPER-SPATIAL RESOLUTION IMAGERY DERIVED from AN UNMANNED AERIAL VEHICLE. *ISPRS Annals of the Photogrammetry, Remote Sensing and Spatial Information Sciences*, *1*(September), 101–106. https://doi.org/10.5194/isprsannals-I-4-101-2012

Lefcheck, J. S., Marion, S. R., Lombana, A. V., & Orth, R. J. (2016). Faunal communities are invariant to fragmentation in experimental seagrass landscapes. *PLoS ONE*, *11*(5), 1–24. https://doi.org/10.1371/journal.pone.0156550

Loarie, S. R., Joppa, L. N., & Pimm, S. L. (2007). Satellites miss environmental priorities. *Trends in Ecology and Evolution*, *22*(12), 630–632. https://doi.org/10.1016/j.tree.2007.08.018

Lyons, M., Roelfsema, C., Kovacs, E., Samper-Villarreal, J., Saunders, M., Maxwell, P., & Phinn, S. (2015). Rapid monitoring of seagrass biomass using a simple linear modelling approach, in the field and from space. *Marine Ecology Progress Series, 530*, 1–14.

McKenzie, L.J. (2003). Draft guidelines for the rapid assessment of seagrass habitats in the western Pacific. Department of Primary Industries Queensland.

McKenzie, L.J., Campbell, S.J. & Roder, C.A. (2003). Seagrass-Watch: Manual for Mapping & Monitoring Seagrass Resources by Community (citizen) volunteers. 2nd Edition. Department of Primary Industries Queensland. http://www.seagrasswatch.org/manuals.html

McRoy, C.P. & C. McMillan. (1977). Production ecology and physiology of seagrasses. In C.P. McRoy and C. Helfferich (Eds.). *Seagrass ecosystems: a scientific perspective* (pp. 53-88). New York: Marcel Dekker.

McGarigal, K. (1995). *FRAGSTATS: spatial pattern analysis program for quantifying landscape structure* (Vol. 351). US Department of Agriculture, Forest Service, Pacific Northwest Research Station.

Moore, K.A. (2009, 2017 (revised)). NERRS SWMP Vegetation Monitoring Protocol: Long-term Monitoring of Estuarine Vegetation Communities. National Estuarine Research Reserve Technical Report: 35 pp.

Nahirnick, N. K. (2018*). Long-term spatial-temporal eelgrass (Zostera marina) habitat change (1932-2016) in the Salish Sea using historic aerial photography and unmanned aerial vehicle*. [Thesis, University of Victoria]. Retrieved from http://dspace.library.uvic.ca/handle/1828/9380\

Nahirnick, N. K., Reshitnyk, L., Campbell, M., Hessing-Lewis, M., Costa, M., Yakimishyn, J., & Lee, L. (2019). Mapping with confidence; delineating seagrass habitats using Unoccupied Aerial Systems (UAS). *Remote Sensing in Ecology and Conservation*, *5*(2), 121–135. https://doi.org/10.1002/rse2.98

NOAA (National Oceanic and Atmospheric Administration). (2012). *State of the science fact sheet: emerging technologies for mobile Earth observations.* https://www.arl.noaa.gov/documents/Summaries/AQSOSFactSheet2012.pdf

Olesen, B., & Sandjensen, K. (1994). Patch dynamics of eelgrass Zostera marina. *Marine Ecology Progress Series*, *106*(1–2), 147–156. https://doi.org/10.3354/meps106147

O'Neill, J. D., & Costa, M. (2013). Mapping eelgrass (Zostera marina) in the Gulf Islands National Park Reserve of Canada using high spatial resolution satellite and airborne imagery. *Remote Sensing of Environment, 133*, 152–167

Pasqualini, V., Pergent, C., Fernandez, C., Pergent, G., Pasqualini, V., Pergent, C., … The, G. P. (2018). The use of airborne remote sensing for benthic cartography : Advantages and reliability To cite this version : HAL Id : hal-01768676.

Phillips, R.C. (1984). *Ecology of eelgrass meadows in the Pacific northwest: A community profile.* U.S. Fish and Wildlife Service.

Reusch, T. B. H., & Williams, S. L. (1998). Variable responses of native eelgrass Zostera marina to a non-indigenous bivalve Musculista senhousia. *Oecologia*, *113*(3), 428–441. https://doi.org/10.1007/s004420050395

Robbins, B. D., & Bell, S. S. (1994). Seagrass landscapes: a terrestrial approach to the marine subtidal environment. *Trends in Ecology & Evolution*, *9*(8), 301-304.

Rumrill, S. S., & Sowers, D. C. (2008). Concurrent Assessment of Eelgrass Beds (Zostera marina) and Salt Marsh Communities along the Estuarine Gradient of the South Slough, Oregon. *Journal of Coastal Research*, *10055*, 121–134. https://doi.org/10.2112/si55-016.1

Rumrill, S. S. (2015). *The Ecology of the South Slough Estuary: Site Profile of the South Slough National Estuarine Research Reserve, Oregon.* South Slough National Estuarine Research Reserve.

Scanlon, T.M., Caylor, K.K., Levin, S.A., Rodriguez-Iturbe, I. (2007) Positive feedbacks promote power-law clustering of Kalahari vegetation. *Nature 449*, 209–213.

Short, F. T., Polidoro, B., Livingstone, S. R., Carpenter, K. E., Bandeira, S., Bujang, J. S., …Zieman, J. C. (2011). Extinction risk assessment of the world's seagrass species. *Biological Conservation*, 144, 1961–1971.

Short, F. T., Muehlstein, L., & Porter, D. (1987). Eelgrass wasting disease: cause and occurence of a marine epidemic. *Biology Bulletin*, *173*, 557–562.

Short, F.T. & Wyllie-Echeverria, S. (1996). Natural and human- induced disturbance of seagrasses. *Environmental Conservation 23*, 17-27.

Short, F.T., McKenzie, L.J., Coles, R.G., Vidler, K.P., Gaeckle, J.L. (2015). SeagrassNet Manual for Scientific Monitoring of Seagrass Habitat, Worldwide edition. University of New Hampshire Publication.

Solé, R. (2011). Phase Transitions. Princeton University Press, Princeton.

Stamey, M. (2004). *An Analysis of Eelgrass Transplantation Performance in Puget Sound, WA, 1990-2000*. [Thesis, University of Washington].

Thom, R., Gaeckle, J., Borde, A., Anderson, M., Boyle, M., Kyte, M., … Wyllie-, S. (2008). *Eelgrass (Zostera marina L .) Restoration in the Pacific Northwest : Recommendations to improve project success*. *U.S. Department of Energy*.

Thom, R. M., Diefenderfer, H. L., Vavrinec, J., & Borde, A. B. (2012). Restoring Resiliency: Case Studies from Pacific Northwest Estuarine Eelgrass (Zostera marina L.) Ecosystems. *Estuaries and Coasts*, *35*(1), 78–91. https://doi.org/10.1007/s12237-011-9430-6

Tiner, R., McGuckin, K., Fields, M., Fuhrman, N., Halavik, T., & MacLachlan, A. (2010). *2009 Eelgrass Survey for Eastern Long Island Sound, Connecticut and New York.* Hadley, MA.

Tuxen, K. A., Schile, L. M., Kelly, M., & Siegel, S. W. (2008). Vegetation colonization in a restoring tidal marsh: A remote sensing approach. *Restoration Ecology*, *16*(2), 313-323.

Uhrin, A. V., & Turner, M. G. (2018). Physical drivers of seagrass spatial configuration: the role of thresholds. *Landscape Ecology*, *33*(12), 2253–2272. https://doi.org/10.1007/s10980-018-0739-4

Ventura, D., Bonifazi, A., Gravina, M. F., Belluscio, A., & Ardizzone, G. (2018). Mapping and classification of ecologically sensitive marine habitats using unmanned aerial vehicle (UAV) imagery and Object-Based Image Analysis (OBIA). *Remote Sensing*, *10*(9), 1–23. https://doi.org/10.3390/rs10091331

Ventura, D., Bruno, M., Lasinio, G. J., Belluscio, A., & Ardizzone, G. (2016). A low-cost drone based application for identifying and mapping of coastal fish nursery grounds. *Estuarine, Coastal and Shelf Science*, *171*, 85-98.

Waycott, M., Duarte, C. M., Carruthers, T. J. B., Orth, R. J., Dennison, W. C., Olyarnik, S., … Williams, S. L. (2009). Accelerating loss of seagrasses across the globe threatens coastal ecosystems. *Proceedings of the National Academy of Sciences of the United States of America*, *106*(30), 12377–12381. https://doi.org/10.1073/pnas.0905620106

Ward, D. H., Morton, A., Tibbitts, T. L., Douglas, D. C., & Carrera-González, E. (2003). Long-term Change in Eelgrass Distribution at Bahía San Quintín, Baja California, Mexico, using Satellite Imagery. *Estuaries*, *26*(6), 1529–1539. https://doi.org/10.1007/BF02803661

Watson, R., Coles, R., Lee Long, W. (1993). Simulation estimates of annual yield and landed value for commercial penaeid prawns from a tropical seagrass habitat. *Australian Journal of Marine and Freshwater Research 44*, 211–219.

Whippo, R., Knight, N. S., Prentice, C., Cristiani, J., Siegle, M. R., & O'Connor, M. I. (2018). Epifaunal diversity patterns within and among seagrass meadows suggest landscape-scale biodiversity processes. *Ecosphere, 9*(1). https://doi.org/10.1002/ecs2.2490

Wicaksono, P., & Hafizt, M. (2013). Mapping seagrass from space: Addressing the complexity of seagrass LAI mapping. *European Journal of Remote Sensing*, *46*(1), 18-39.

Wirfs, K. and A. Helms. 2018. Case of the Disappearing Eelgrass. National Science Foundation, Research Experience for Undergraduates, Exploration of Marine Biology on the Oregon Coast fellowship program (NSF REU EMBOC). Poster presentation 8/15/18, University of Oregon, Oregon Institute of Marine Biology, Charleston, OR.

Woodcock, C.E. & Strahler, A.H. (1987). The Factor of Scale in Remote-Sensing. *Remote Sensing of the Environment 21,* 311-332.

van der Heide, T., van Nes, E. H., Geerling, G. W., Smolders, A. J. P., Bouma, T. J., & van Katwijk, M. M. (2007). Positive Feedbacks in Seagrass Ecosystems: Implications for Success in Conservation and Restoration. *Ecosystems*, *10*(8), 1311–1322. https://doi.org/10.1007/s

Young, D., Clinton, P., Specht, D., Mochon Collura, T. C., & Lee, H. (2012). Determining bathymetric distributions of the eelgrass Zostera marina L. in three turbid estuaries on the eastern North Pacific coast. *Botanica Marina*, *55*(3), 229–240. https://doi.org/10.1515/bot-2011-0011

Yednock, B., & QSI Corvallis. (2017). *Coos Estuary, Oregon Orthophotography and Eel Grass Feature Extraction Technical Data Report - Revised*.

Yu, Q., Yu, Q., Gong, P., Clinton, N., Biging, G., Kelly, M., & Schirokauer, D. (2006). Objectbased detailed vegetation classification with airborne high spatial resolution remote sensing imagery. Photogrammetric Engineering and Remote. *Photogrammetric Engineering & Remote Sensing*, *72*(7), 799–811.

Zhang, H., Fritts, J. E., & Goldman, S. A. (2008). Image segmentation evaluation: *A survey of unsupervised methods. computer vision and image understanding*, *110*(2), 260-280.